

Response to the Comments of Referees

RH and O₃ concentration as two prerequisites for sulfate formation

Yanhua Fang and Chunxiang Ye, Junxia Wang, Yusheng Wu, Min Hu, Weili Lin, Fanfan Xu, Tong Zhu

We thank the referees for the critical comments, which are very helpful in improving the quality of the manuscript. We have made major revision based on the critical comments and suggestions of the referees. Our point-by-point responses to the comments are listed in the following.

Anonymous Referee #1

Received and published: 9 May 2019

Comment NO.1: *The manuscript by Fang et al. provides a nice year-long dataset of PM_{2.5} along with chemical composition and some important precursors, which would be of interest in improving the understanding of pollution evolution in Beijing. Throughout the manuscript, the authors focused mostly on the observed relationships between SOR and O₃/RH, and made conclusions that O₃ and RH are two “prerequisites” of sulfate formation. These conclusions, however, are predictable. RH and O₃ together provide almost all the necessary conditions for sulfate formation: for gas phase oxidation, they are sources of OH, and for aqueous phase or heterogeneous phase oxidations, water and oxidants (O₃, H₂O₂ (O₃ was a precursor of H₂O₂)).*

This is saying, that the authors focused on the relationship between SOR and O₃/RH and concluded on multi-phase reaction by H₂O₂ oxidation dominate (or major) sulfate formation is over concluded, or more like a speculation, especially given the absence of H₂O₂ data.

In addition, there should be seasonal difference on the formation route, for example, in summer, pollution was the lowest and SOR was the highest, given the data presented, one cannot judge that multi-phase reaction by H₂O₂ oxidation should be responsible for sulfate formation: won't the gas-phase oxidation also enhanced in summer? In fact, for multiphase reactions, AWC might be a better indicator, however, as shown in Figure 7, SOR is not well correlated with AWC but better with RH. This for me is a good if not strong indicator that gas-phase oxidation (promoted by high O₃ + RH + insulation) is important for at least summer high SOR.

Response:

We are grateful to the reviewer for the positive and encouraging comments on the dataset and the scientific

contribution of our manuscript to understanding sulfate formation.

- 1) We would like to first summarize the main contribution of our manuscript here. Our manuscript is the first to introduce the idea that there are some threshold values (or turning points), above which the SOR increases rapidly, for both RH and O₃, based on year-long observations. We presented clear observational evidence for these thresholds, best seen in the plot of SOR versus RH and O₃ data (Fig. 5 in the revised manuscript, Page 25). The thresholds at roughly 35 ppb O₃ and 45 % RH are observed. Although such turning point possibly varies in different seasons and locations, such thresholds immediately indicate that both RH and O₃ are two “prerequisites” for the multiphase formation of sulfate. In the case of the RH threshold, this is consistent with current understanding in the dependence of the multiphase sulfate formation on aerosol water, since RH threshold relates to the semisolid-to-liquid phase transition of atmospheric aerosols. Correlation analysis between SOR and AWC further backs this point up (Fig. R1 in this response, which has been added to the revised SI as Fig. S3, Page 37). In the case of O₃ concentration threshold, this is consistent with the consumption of liquid oxidants in multiphase sulfate formation.
- 2) We agree with the referee that lack of H₂O₂ measurement is a weakness in the discussion of possible role of H₂O₂ in sulfate formation mechanisms. To add more confidence in such discussion, a proxy measurement of H₂O₂ is included in the revised manuscript. Taking the advice of Referee #1 (comment NO.4), that H₂O₂ was non-linearly correlated with temperature (Fu, 2014). H₂O₂ was estimated from temperature, by assuming the same relationship applicable to our measurements in the full year of 2012–2013. As shown in Fig. R2 in the response to Referee #1 comment 4 (added in the revised SI as Fig. S6, Page 39), maximum concentration of H₂O₂ in summer is expected and confirmed, which is in line with the fastest sulfate formation in summer all over the year. SOR was further plotted against H₂O₂ and positive correlation was found between them (in the response to Referee #1 comment 4, added in the revised SI as Fig.S7, Page 40). In addition, coincident increases in the concentration of H₂O₂ and PM_{2.5} in winter of Beijing also lead to an important role of the H₂O₂ route in sulfate formation (Ye et al., 2018). These discussions were added up to our previous analysis in the original manuscript, i.e., O₃ and H₂O₂ are proposed to be the major oxidants in multiphase sulfate formation based on the above threshold analysis. Since O₃ was excluded as a major oxidant in multiphase sulfate formation, for that the high aerosol acidity in urban environments limits its reaction rate, H₂O₂ remains the only possible liquid phase oxidant. Based on all the above discussions, we

carefully proposed in the revised manuscript that H₂O₂ might be an important oxidant of sulfate formation.

- 3) As reminded by Referee #1, we double-checked the relationship between SOR and AWC (Fig. R1 in this response, added in the revised SI as Fig. S3, Page 37), and positive correlation between them was found, which further supports that the multiphase reactions, rather than gas phase reactions, are responsible for sulfate formation.
- 4) The possible role of gas phase reactions was further discussed in the revised manuscript. First, the thresholds of O₃ and RH are suggestive of multiphase reactions, as stated above, rather than gas phase reactions, to account for sulfate formation. Second, coincident increases in SOR with aerosol loading (Fig.11 in the revised manuscript, Page 31), with concomitant suppression of photochemistry due to light shielding by aerosols (Wang et al., 2017) and NO-titration of O₃ (Page 8 line 201 in the revised manuscript), excludes gas phase reactions as a major route of sulfate formation in Beijing. Last but not the least, gas phase reactions may contribute but are not the major route of sulfate formation, either in Beijing or globally, due to the relatively slow reaction of SO₂ with OH. For example, the lifetime of SO₂ with respect to OH oxidation is about 3–4 days, assuming a 24-h average OH concentration of 1×10^6 molecules cm⁻³ and a pseudo-secondary-order rate constant of 10^{-12} cm³ molecules⁻¹ s⁻¹ (Brothers et al., 2010). However, the overall oxidation lifetime of SO₂ is on the order of hours (Berglen et al., 2004; He et al., 2018). Hence, that gas phase reactions contribute but are not the major route of sulfate formation is a well-accepted point in the literature (Finlayson-Pitts and Pitts, 2000; He et al., 2018).

However, we agree with the reviewer that gas phase reactions cannot be neglected and that the gas phase reaction competes with multiphase reactions in sulfate formation. For example, both O₃ and RH/water vapor concentration increased in summer with pollution accumulation. As the precursors of OH radicals, the increasing trends of both O₃ and water vapor might indicate increasing concentration of OH, and hence reaction rate of SO₂ and OH. A discussion of the possible role of gas phase reactions has been added to Page 11 lines 311–319 in the revised manuscript.

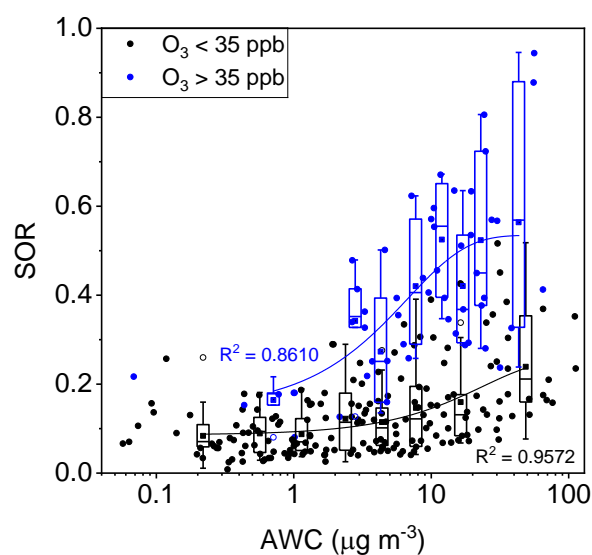


Figure R1. Plot of the sulfur oxidation ratio (SOR) against aerosol water content (AWC) (note log scale), grouped by O_3 concentration. The solid blue circles represent $O_3 > 35$ ppb and the solid black circles represent $O_3 < 35$ ppb. The boxes represent, from top to bottom, the 75th, 50th, and 25th percentiles in each bin, which were also separated according to the 35 ppb O_3 concentration threshold; the bin widths were set such that there were an approximately equal number of data points in each bin. The whiskers, solid squares, and open circles represent 1.5 times the interquartile range (IQR), mean values, and outlier data points, respectively. The lines are best fits to the mean values based on a sigmoid function. Data for days with rain or snow were excluded from this plot.

Changes in Manuscript: As for the discussion on H_2O_2 oxidation, please refer to the revised manuscript, Page 6 lines 169–170 and Page 9 lines 230–245. For the discussion on gas reaction, please refer to the revised manuscript, Page 11 lines 311–319.

Comment NO.2: *The fact of no correlation between SOR and NO_2 could make a good argument on the role of NO_2 in sulfate formation, I suggest to emphasize this point. In addition, comparing SOR, NO_2 and NH_4^+ (it would be better if NH_3 is available), and see if there is any clue on the role of NH_3 in aerosol pH and the promoted NO_2 oxidation route as proposed by earlier studies.?*

Response:

We took the advice and further discussed the possible role of NO_2+O_2 route in the revised manuscript based on the following two points. First, no correlation between the SOR and NO_2 was found. Secondly, although in our study, NH_3 measurements were not available, previous studies have reported a mean aerosol pH value of 4.2 with a low limit of 3.0 in Beijing (Ding et al., 2019; Liu et al., 2017a), which suggests that several pH-sensitive routes of sulfate formation, such as $NO_2 + O_2$, TMI + O_2 , O_3 etc., are highly suppressed. Therefore, we proposed that NO_2+O_2 might not be a major mechanism of sulfate

formation.

Changes in Manuscript: Please refer to the revised manuscript, Page 9 lines 245–259 and Page 10 lines 260–261.

Comment NO.3: *It looks the authors dealt with SOR as a sole local phenomenon (local emission and local oxidation), but how about the difference in the regional transport of SO₂ and SO₄²⁻? What would this do to SOR?*

Response:

Yes, regional transport or intrusion of SO₂ and SO₄²⁻ into Beijing has been evidenced in the literature (Lang et al., 2013; Li et al., 2016), and would contribute to SOR. However, our analysis was based on stationary measurements and regional transport could not be considered based on the data we have. Even though, strong relationships between SORs and RH/O₃ were still found, revealing the dominant role of Local multiphase reactions in sulfate formation. Further chemical-transport model study in the future is encouraged to more accurately evaluate the contribution of local chemical formation to sulfate.

Changes in Manuscript: Uncertainty analysis introduced from neglecting regional transport has been added to the revised manuscript, Page 3 lines 60–63.

Comment NO.4: *There is observational data on the relationship of H₂O₂ concentration and temperature in Beijing (Fu, A.: Study on peroxides concentration and its influencing factors in the urban atmosphere, master of engineering, College of Environmental and Resource Sciences, Zhejiang University, Hangzhou, China, 56 pp., 2014 (in Chinese)), the authors can derive the H₂O₂ concentration from the temperature data to better constrain the role of H₂O₂ by comparisons with O₃ and SOR data.*

Response: Accepted

According to Fu (2014), H₂O₂ was non-linearly correlated with temperature. By assuming the same relationship applicable to our measurements in the full year of 2012–2013, H₂O₂ was estimated from temperature and shown in Fig. R2 in this response (added to the revised SI as Fig. S6, Page 39). Maximum concentration of H₂O₂ in summer is expected and confirmed, which is in line with the fastest sulfate formation in summer all over the year.

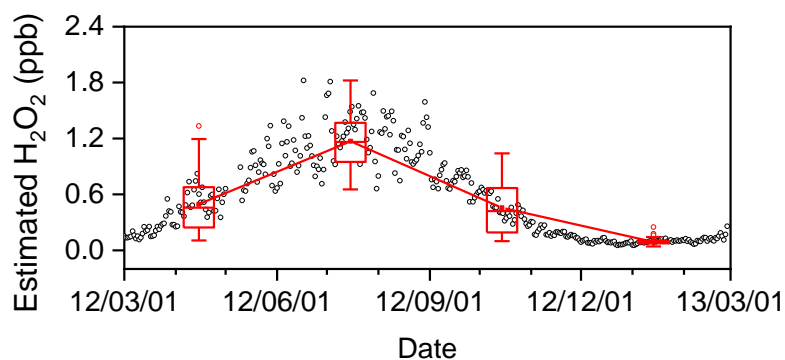


Figure R2. Time series of estimated H_2O_2 from March 1 2012 to February 28 2013 (open black circles). H_2O_2 was estimated from temperature (T) based on the fitting function $\text{H}_2\text{O}_2 = 0.1155e^{0.0846T}$ according to Fu (2014). The boxes represent, from top to bottom, the 75th, 50th, and 25th percentiles for each season. The whiskers, solid red squares, and open red circles represent 1.5 times the interquartile range (IQR), seasonal mean values, and outlier data points, respectively.

SOR was further plotted against H_2O_2 and positive correlation was found between them (Fig. R3 in this response, added to the revised SI as Fig. S7, Page 40), provides more confidence in our discussion of possible role of H_2O_2 oxidation in sulfate formation.

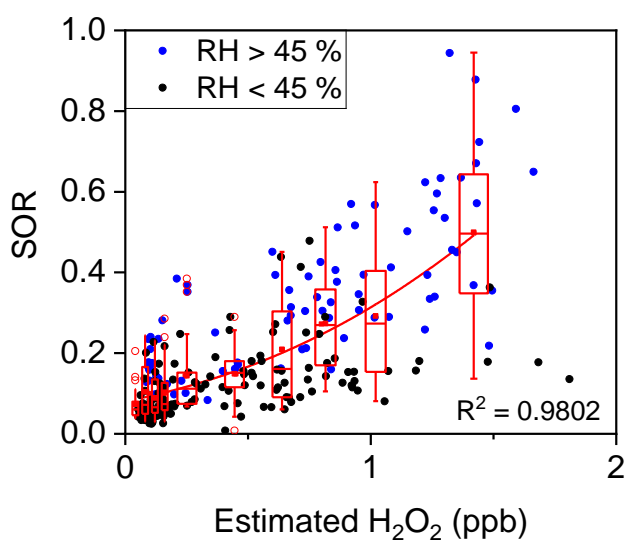


Figure R3. Plot of the SOR against estimated H_2O_2 grouped by RH. The solid blue circles represent $\text{RH} > 45\%$ and the solid black circles represent $\text{RH} < 45\%$. The boxes represent, from top to bottom, the 75th, 50th, and 25th percentiles in each bin. The bin widths were set such that there were an approximately equal number of data points in each bin. The whiskers, solid squares, and open circles represent 1.5 times the IQR, mean values, and outlier data points, respectively. The line are best fits to the mean values based on an exponential function. Data for days with rain were excluded from this plot.

Changes in Manuscript: The proxy measurement of H_2O_2 and further discussion have been added into our revised manuscript, Page 9 lines 230–245.

Comment NO.5: Atmospheric oxidation capacity is a rather vague (or big) definition when related to specific oxidation route of chemicals. Try to avoid

Response: Accepted.

Changes in Manuscript: Atmospheric oxidative capacity was replaced by the appropriate oxidants. Please refer to the revised manuscript, Page 7 line 197, Page 11 line 291, Page 12 lines 323 and 342.

Comment NO.6: *The manuscript need a little bit more tuned, e.g., line 31-32: what is “a given RH threshold”?*

Response: Accepted.

A given RH threshold” refers to RH threshold of around 45% observed in our study.

Changes in Manuscript: We have rewrite the sentence to “when RH was above a threshold of 45%”, please refer to the revised manuscript, Page 6 line 168.

Anonymous Referee #2

Received and published: 29 April 2019

Comment NO.1: *The paper deals with the mass concentration and chemical composition of PM_{2.5} in Beijing during 1 year from filter samples and its correlation with pollution classes (clear days, slight, light, medium and heavy pollution). Most of the paper is devoted to the two prerequisites for sulfate formation based discussion. This is certainly a positive feature of the paper. Although the article has a clear logical structure, I strongly recommend to make the text more concise, to clarify statements, and to delete redundancies.*

Response: Accepted.

We deleted redundancies and clarified several statements based on the referee’s suggestions to make the text more concisely.

Changes in Manuscript: We have deleted redundancies in abstract and section 3.1, please refer to the revised manuscript, Page 1 lines 15–29 and Page 6 lines 149–158. We have replaced the atmospheric oxidation capacity to appropriate oxidant, please refer to the revised manuscript, Page 7 line 197, Page 11 line 291, Page 12 lines 323 and 342. Please also refer to the comments NO.5, NO.9, and NO.12 below.

Comment NO.2: *Most importantly, in the absence of data on hydrogen peroxide, all speculation seems weak. The main idea of the article is still in the cognition of previous studies, and no more innovative conclusions have been put forward. In a word, this article is full of paradoxical conclusions and cannot*

provide a powerful help to the scientific community. Therefore, I don't recommend the publication in ACP journal in current status.

Response: We have made major revision of our manuscript, concerning the following two points:

- 1) We would like to first summary the main contribution of our manuscript here. Our manuscript is the first to introduce the idea that there are some threshold values (or turning points), above which the SOR increases rapidly, for both RH and O₃, based on year-long observations. We presented clear observational evidence for these thresholds, best seen in the plot of SOR versus RH and O₃ data (Fig. 5 in the revised manuscript, Page 25). The thresholds at roughly 35 ppb O₃ and 45 % RH are observed. Although such turning point possible varies in different seasons and locations, such thresholds immediately indicate that both RH and O₃ are two “prerequisites” for the multiphase formation of sulfate. In the case of the RH threshold, this is consistent with current understanding in the dependence of the multiphase sulfate formation on aerosol water, since RH threshold relates to the semisolid-to-liquid phase transition of atmospheric aerosols. Correlation analysis between SOR and AWC further backs this point up (Fig. R1 in the response to Referee # 1 comment NO.1, added to the revised SI as Fig. S3, Page 37). In the case of O₃ concentration threshold, this is consistent with the consumption of liquid oxidants in multiphase sulfate formation.
- 2) We agree with the referee that lack of H₂O₂ measurement is a weakness in the discussion of possible role of H₂O₂ in sulfate formation mechanisms. To add more confidence in such discussion, a proxy measurement of H₂O₂ is included in the revised manuscript. Taking the advice of Referee #1, that H₂O₂ was non-linearly correlated with temperature (2014). H₂O₂ was estimated from temperature, by assuming the same relationship applicable to our measurements in the full year of 2012–2013. As shown in Fig. R2 (in the response to Referee # 1 comment NO.4, added in the revised SI as Fig. S6, Page 39), maximum concentration of H₂O₂ in summer is expected and confirmed, which is in line with the fastest sulfate formation in summer all over the year. SOR was further plotted against H₂O₂ and positive correlation was found between them (Fig. R3 in the response to Referee # 1 comment NO.4, added in the revised SI as Fig.S7, Page 40.). In addition, coincident increases in the concentration of H₂O₂ and PM_{2.5} in winter of Beijing also lead to an important role of the H₂O₂ route in sulfate formation (Ye et al., 2018). These discussions were added up to our previous analysis in the original manuscript, i.e., O₃ and H₂O₂ are proposed to be the major oxidants in multiphase sulfate formation based on the above threshold analysis. Since O₃ was excluded as a major oxidant in

multiphase sulfate formation, for that the high aerosol acidity in urban environments limits its reaction rate, H₂O₂ remains the only possible liquid phase oxidant. Based on all the above discussions, we carefully proposed in the revised manuscript that H₂O₂ might be an important oxidant of sulfate formation.

Changes in Manuscript: A summary of our scientific contribution has been revised in the abstract, please refer to the revised manuscript, Page 1 lines 14–29. Further discussions on the role of H₂O₂ has also been added to the revised manuscript, Page 9 lines 230–245.

Comment NO.3: *The author name should be Weili Lin.*

Response: Accepted.

Changes in Manuscript: We have made a correction, please refer to the revised manuscript, Page 1 line 2.

Comment NO.4: *"threshold of RH and ozone" Where is this statement coming from? Is it a definition/estimate of the authors? If the threshold changed with different locations and seasons? What is the effect of these thresholds?*

Response:

- 1) “Thresholds of RH and ozone” are obtained based our measurement in the full year of 2012-2013 that above some turning points of RH and O₃ concentration, SORs increase rapidly. This is best seen in the plot of SOR versus RH and O₃ data (Fig. 5 in the revised manuscript, Page 25). Our interpretation of this is that there are thresholds or turning points in RH and O₃ concentration that must be exceeded to allow for the fast formation of sulfate. Although such turning point possible varies in different seasons and locations, such thresholds immediately indicate that both RH and O₃ are two “prerequisites” for the multiphase formation of sulfate.
- 2) It is also the authors’ interpretation that the threshold of RH is around 45 % and the threshold of O₃ is around 35 ppb. There could be some uncertainty attached with such inferred values. For example, one could argue that the threshold of O₃ concentration is any value between 30–40 ppb. Also, the daily average RH and O₃ data used in our analyses are not the best to evaluate the thresholds. For example, the observed RH threshold is proposed to be determined by the phase transition RH. However, the timescale of the phase transition in ambient air is on the order of seconds (Liu et al., 2008), in

comparison to RH changes on timescales of hours to days, and thus the daily average RH is not an accurate estimate of the phase transition RH. This explains why the apparent RH threshold of 45 % observed in Fig. 5 (Page 25 in the revised manuscript) is somewhat below the *in situ* phase transition RH of 50–60 % (Liu et al., 2017b).

- 3) The thresholds might change with locations and seasons. For instance, Fig. R4 in this response (added to the revised manuscript as Fig. 6, Page 26) suggests that the RH threshold is roughly around 45 % during all four seasons in Beijing. The turning point varied within 40 %–50 % in different sampling location of Beijing (Liu et al., 2015; Xu et al., 2017; Yang et al., 2015; Zheng et al., 2015). However, similar analyses must be performed using high time resolution data to confirm the trends observed based on our daily average data.

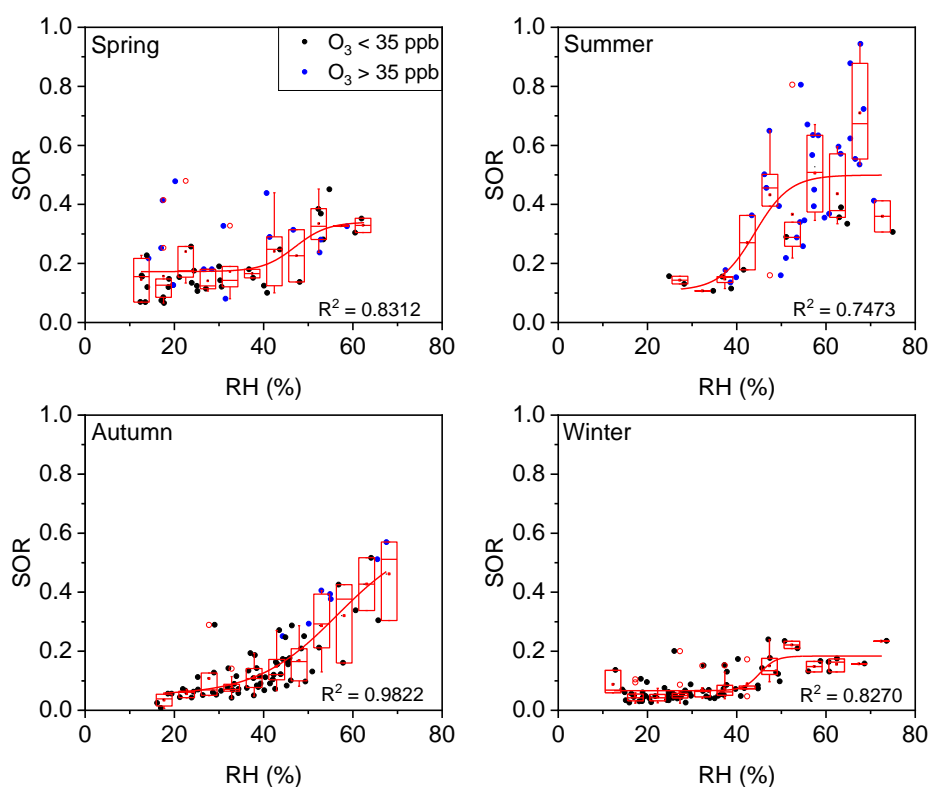


Figure R4. Plots of SORs against RH, grouped by O₃ concentration in four seasons. The solid blue circles represent O₃ > 35 ppb and the solid black circles represent O₃ < 35 ppb. The boxes represent, from top to bottom, the 75th, 50th, and 25th percentiles in each bin (Δ RH = 5 %). The whiskers, solid red squares, and open red circles represent 1.5 times the IQR, mean values, and outlier data points, respectively. The red lines are best fits to mean values based on sigmoid function. Data for days with rain or snow were excluded from these plots.

- 4) As stated above, above the thresholds of RH and O₃ concentration, sulfate formation could be enhanced (Please also refer to the response to Referee #2 comment NO.2).

Changes in the Manuscript: A discussion on the possible seasonal variations in the thresholds were added in our revised manuscript, please refer to the revised manuscript, Page 8 lines 215–223.

Comment NO.5: *Redundancy: Page 1 line 15-16 and line 24-25. Line 13-14 and Line 17-18.*

Response: Accepted.

Changes in the Manuscript: We have rewritten the abstract and deleted the redundant sentences in the revised manuscript. Please refer to the revised manuscript, Page 1 lines 14–29.

Comment NO.6: *Section 2.1.2. Please add the steps of weighing after sampling.*

Response:

The steps of weighting after sampling have been provided in the original manuscript. Please also refer to the revised manuscript, Page 4 lines 109–110 (highlighted).

Comment NO.7: *Page 4, line 27. Should be annual standard*

Response: Accepted.

Changes in Manuscript: We have changed the phrase to “Chinese National Ambient Air Standard annual mean concentration of”, please refer to the revised manuscript, Page 6 line 147.

Comment NO.8: *Page 5, line 2. The method to calculate POM should be introduced in previous section.*

Response:

The method to calculate POM was provided in the original SI. The discussion on source appointment, including POM, has been deleted in the revised manuscript and SI.

Comment NO.9: *Overall, section 3.1 is not necessary, because it has nothing to do with the main idea. If this section is deleted in the main article, it will not affect the presentation of the article. For example, the authors described the measurements of ions, organics and metal. However, ions except SNA, organics and metals except Fe didn't help the discussion of your topic. Therefore, the method and results section should to be streamlined.*

Response: Accepted

Changes in Manuscript: Sect 3.1 has been reduced so that a general description of data is presented, and that variations in PM_{2.5} and its main components are introduced. Please refer to the revised manuscript,

Page 6 lines 144–161.

Comment NO.10: *Section 3.2. I strongly recommend the authors discussing the relationship between sulfate and RH/ozone in different seasons. The threshold should be changed with seasons.*

Response: Accepted

Changes in Manuscript: The seasonal variations are discussed now in the revised manuscript. Please refer to the revised manuscript, Page 8 lines 215–223.

Comment NO.11: *Page 7, line 12-16 repeats the previous statement.*

Response:

We intended to summarise our major findings and discuss their implications in this section.

Changes in Manuscript: We have rewritten the sentences, please refer to the revised manuscript, Page 9 lines 230–232.

Comment NO.12: *Page 7, line 14. What is the atmospheric oxidative capacity? From your statement, does ozone concentration correspond to this? Is it correct? Do you have some references to support your opinion? The authors should clarify this question because the same definition is also used in Page 9, line 20.*

Response: Accepted.

Atmospheric oxidative capacity relates to the concentrations of major oxidants such as OH radicals, O₃, etc. (Murray et al., 2009). Since O₃ is a major oxidant and a precursor to other major oxidants, including OH radicals, to a certain degree, O₃ can be used as a proxy for atmospheric oxidative capacity. To improve clarity, atmospheric oxidative capacity was replaced by the appropriate oxidant in each context in the revised manuscript.

Changes in Manuscript: Atmospheric oxidative capacity was replaced by the appropriate oxidant. Please refer to the revised manuscript, Page 7 line 197, Page 11 line 291, Page 12 lines 323 and 342.

Comment NO.13: *Page 7, Line 23-24. Since you couldn't exclude NO₂-based reactions as major route of sulfate formation, the analysis of the relationship between SOR and NO₂ is not necessary.*

Response:

We took the advice of Referee #1 and further discussed the possible role of NO_2+O_2 route in the revised manuscript based on two points. First, no correlation between the SOR and NO_2 was found. Secondly, although in our study, NH_3 measurements were not available, previous studies has reported a mean aerosol pH value of ~ 4.2 with a low limit of ~ 3.0 in Beijing (Ding et al., 2019; Liu et al., 2017a), which suggests that several routes of sulfate formation, such as $\text{NO}_2 + \text{O}_2$, TMI + O_2 , O_3 etc., are suppressed. Therefore, we proposed that NO_2+O_2 might not be a major mechanism of sulfate formation.

Changes in Manuscript: Please refer to the revised manuscript, Page 9 lines 247–259 and Page 10 lines 260–261.

Comment NO.14: *Page 9, line 2-3. The authors described on page 7, line 7-10 that the self-catalytic nature is beyond the scope of your study. However, you illustrate the importance of the self-catalytic in this paragraph. I think it's self-contradictory.*

Response:

To clarify, our manuscript states that the self-constrained nature, i.e., sulfate formation increases the acidity of aerosols, which suppresses sulfate formation via several routes, such the O_3 oxidation and TMI + O_2 routes. The self-catalytic nature of sulfate formation is best seen from the perspective that sulfate formation adds up the aerosol volume/surface density which helps with further sulfate formation. Those two mechanisms compete in determining the sulfate formation as pollution accumulation. In our manuscript, the self-constrained nature of sulfate formation is not discussed in detail due to the lack of direct or proxy measurements of aerosol acidity in our measurements.

Comment NO.15: *Page 10, line 21. Should be Zhejiang University.*

Response: Accepted.

Changes in Manuscript: We have made the correction. Please refer to the revised manuscript, Page 14 lines 388.

Anonymous Referee #3

Received and published: 12 May 2019

Comment NO.1: *General points: This study provides long-term continuous filter sampling and composition analysis data of $\text{PM}_{2.5}$. Many previous studies usually conducted such kind of observation intermittent for a short period, but such long-term uninterrupted observations are quite scarce. Thus, the*

data is of scientific value for analysis of variation characteristics of PM_{2.5} compositions and model validation. Moreover, this paper focus on identifying the possible factors on sulfate formation, which is helpful for understanding of mechanism of sulfate formation. If the general and specific points below are addressed, I recommend this paper for publication.

The authors investigate the relationship of SOR and RH/O₃, and conclude that RH and O₃ are two “prerequisite” for sulfate formation. But the further speculation of “H₂O₂ oxidation was proposed to be the major route” seems lack of sufficient evidence without the H₂O₂ data and laboratory experiment results support. The refs. (Sievering et al. 2004; Alexander et al., 2005) are also not solid enough to back your speculation.

Response: We are grateful to the reviewer for the positive and encouraging comments on the dataset and the scientific contribution of our manuscript to understanding sulfate formation.

We agree with the referee that lack of H₂O₂ measurement is a weakness in the discussion of possible role of H₂O₂ in sulfate formation mechanisms. To add more confidence in such discussion, a proxy measurement of H₂O₂ is included in the revised manuscript. Taking the advice of Referee #1, that H₂O₂ was non-linearly correlated with temperature (2014). H₂O₂ was estimated from temperature, by assuming the same relationship applicable to our measurements in the full year of 2012–2013. As shown in Fig. R2 (in the response to Referee # 1 comment NO.4, added in the revised SI as Fig. S6, Page 39), maximum concentration of H₂O₂ in summer is expected and confirmed, which is in line with the fastest sulfate formation in summer all over the year. SOR was further plotted against H₂O₂ and positive correlation was found between them (Fig. R3 in the response to Referee # 1 comment NO.4, added in the revised SI as Fig.S7, Page 40.). In addition, coincident increases in the concentration of H₂O₂ and PM_{2.5} in winter of Beijing also lead to an important role of the H₂O₂ route in sulfate formation (Ye et al., 2018). These discussions were added up to our previous analysis in the original manuscript, i.e., O₃ and H₂O₂ are proposed to be the major oxidants in multiphase sulfate formation based on the above threshold analysis. Since O₃ was excluded as a major oxidant in multiphase sulfate formation, for that the high aerosol acidity in urban environments limits its reaction rate, H₂O₂ remains the only possible liquid phase oxidant. Based on all the above discussions, we carefully proposed in the revised manuscript that H₂O₂ might be an important oxidant of sulfate formation.

Changes in Manuscript: Discussions on the role of H₂O₂ has also been added to the revised manuscript,

Page 9 lines 230–245.

Comment NO.2: *The authors should adjust the structures of the paper to make more clear and concise statement. Although the overview of the data is needed for the readers, the discussion in Sect3.1 is concentrated on the source appointment of PM_{2.5}, which is abundant and deviate away from the theme. I suggest this Sect. discuss the variations of the components concentrations and contribution ratios using the classification method based on season or pollution levels. Sulfate can be focused on.*

Response: Accepted

Changes in Manuscript: Sect 3.1 has been reduced so that a general description of data is presented, and that variations in PM_{2.5} and its main components are introduced. Please refer to the revised manuscript, Page 6 lines 144–161.

Comment NO.3: *The order of the figures and tables in the main text and SI is confusing, the authors should rearrange the figures and tables according to the main text.*

Response: Accepted

Changes in Manuscript: We have rearranged the figures. Please refer to the revised manuscript, Pages 23–24 Figs 3 and 4. Please also refer to the revised SI, Pages 34–35 Figs. S1 and S2.

Comment NO.4: *The authors should carefully go through the whole manuscript to avoid mistakes. Specific points: 1. Avoid duplicated sentences and definitions. E.g. Page1, line18- 20 vs Page 2, line 1-2; Page 1, line 25-26 vs Page2, line 23-26, and the definition of “self-catalytic” is vague.*

Response: Accepted

- 1) Duplicated sentences deleted in the revised manuscript.
- 2) We need to better define the term “self-catalytic” as Referee #2 has also suggested. We have therefore defined it consistently in both the abstract and introduction. The definition has changed to: “the formation of hydrophilic sulfate aerosols under high RH conditions results in an increase in aerosol water content, which results in greater particle volume for further multiphase sulfate formation”.

Changes in Manuscript: The definition has been clarified, please refer to the revised manuscript, Pages 1–2 lines 30–32 and Page 2 lines 52–54.

Comment NO.5: *Page 2, line 14, what is “various parameters” refer to*

Response: oxidants, catalysts, meteorological conditions, etc.

Changes in Manuscript: We have clarified the parameters as “exactly how do various parameters (oxidants, catalysts, meteorological conditions, etc.) influence sulfate formation” in the revised manuscript, Page 2 line 43–44.

Comment NO.6: *Page 4, line 6, Figure 1 should be “Fig. 1”; Page 4, line 15, give the location information (lat, long) of the site; Page 5, line 4-10, rewrite the first sentence “The chemical. . . . (TEOs).” There actually 8 categories including “others” and the category is not according to the source type. Why you start with Fig. S2 not S1? Page 6 why you put Fig. 4 before Fig.3 in your text. Check the orders as mentioned in general points 3.*

Response: Accepted.

Changes in Manuscript:

- 1) Figure 1 has been changed to Fig. 1. Please refer to the revised manuscript, Page 4 line 96.
- 2) The lat/long of the Beijing Meteorological Observatory Station (116.47° E, 39.81° N) has been added. Please refer to the revised manuscript, Page 4 line 104.
- 3) The sentence the reviewer mentions has been rewritten to: “The chemical components of PM_{2.5} were divided into eight categories: sulfate, nitrate, ammonium, organic matter (OM), EC, minerals, trace element oxides (TEOs), and others.” Please refer to the revised manuscript, Page 5 lines 121–122.
- 4) We have rearranged the order of figures. Please refer to the revised manuscript, Pages 5 lines 125–125 and Pages 23–24 Figs 3 and 4.

Comment NO.7: *Sect. 3.2 How do you give the definition of threshold? The SOR or Δ SOR exceed certain value? The authors also compared the results with previous studies in this Sect., what is the reason for the difference in these studies?*

Response:

- 1) “Thresholds of RH and ozone” are obtained based our measurement in the full year of 2012-2013 that above some turning points of RH and O₃ concentration, SORs increase rapidly. This is best seen in the plot of SOR versus RH and O₃ data (Fig. 5 in the revised manuscript, Page 25). Our interpretation of this is that there are thresholds or turning points in RH and O₃ concentration that must be exceeded to allow for the fast formation of sulfate. Although such turning point possible

varies in different seasons and locations, such thresholds immediately indicate that both RH and O₃ are two “prerequisites” for the multiphase formation of sulfate.

2) It is also the authors’ interpretation that the threshold of RH is around 45 % and the threshold of O₃ is around 35 ppb. There could be some uncertainty attached with such inferred values. For example, the thresholds might change with locations and seasons. Also, the daily average RH and O₃ data used in our analyses are not the best to evaluate the thresholds. For example, the observed RH threshold is proposed to be determined by the phase transition RH. However, the timescale of the phase transition in ambient air is on the order of seconds (Liu et al., 2008), in comparison to RH changes on timescales of hours to days, and thus the daily average RH is not an accurate estimate of the phase transition RH. This explains why the apparent RH threshold of 45 % observed in Fig. 5 (Page 25 in the revised manuscript) is somewhat below the *in situ* phase transition RH of 50–60 % (Liu et al., 2017b).

Comment NO.8: *Page 9, line 5-8 and Page 9, line 12-14 the sentences are contradictory*

Response:

The sentences on Page 9, lines 5–8 explain that the self-catalytic nature of sulfate formation accounts for the increased SOR as pollution accumulates. The sentences on page 9, lines 12–14 summarise our conclusion about the thresholds of O₃ and RH.

Comment NO.9: *Use “clear”, “formation”, “evolution” etc. to represent different pollution level is improper, because you do not conduct case or course study in the paper.*

Response: Accepted.

Changes in Manuscript: The definitions have been changed to: clean, moderate pollution, heavy pollution, and severe pollution in the revised manuscript. Please refer to the revised manuscript, Page 11 lines 299–300, Page 30 lines 606–607, and Page 31 lines 609–610. These still represent each quartile of PM_{2.5} levels.

Comment NO.10: *How about other factors such as wind speed and wind direction impact on SOR except RH and O₃?*

Response:

Wind speed and wind direction are not assumed to be influencing parameters of sulfate formation according to the mechanism summarised in the introduction section and hence were not discussed in our

manuscript. However, it is clear that high SORs and high PM_{2.5} were commonly found at low to medium wind speeds (Fig. R5 in this response), which might be related to the increasing SORs as aerosol pollution accumulated. Hotspots of SOR at high wind speed with northwest sector and south sector are also found, which might be related to regional transport of sulfate. The uncertainty concerning regional transport has been discussed in the response to Referee #1 comment NO.3.

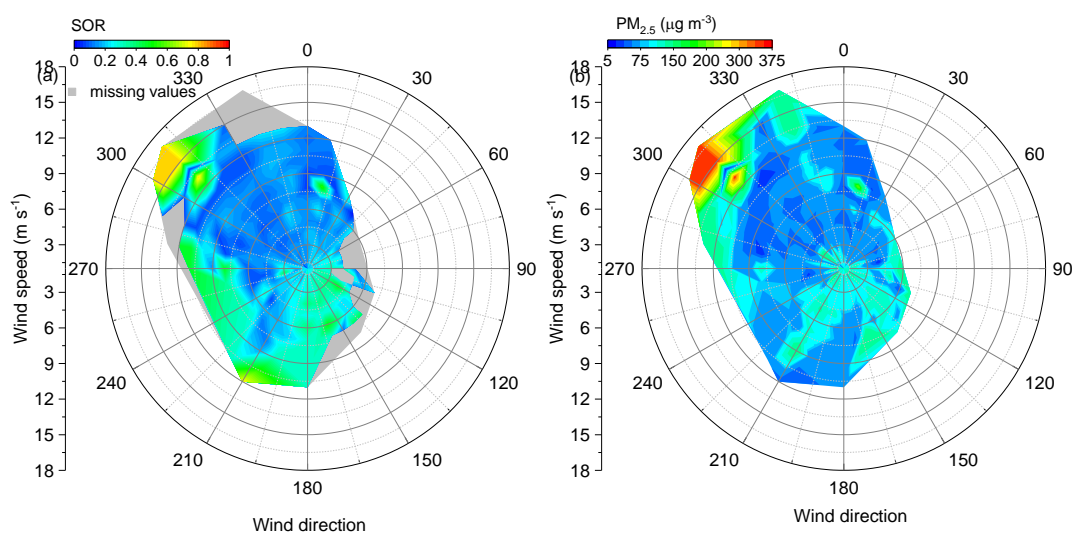


Figure R5. Bivariate polar plots for (a) SOR and (b) PM_{2.5}. The grey shading indicates lack of data. Wind speed and wind direction were download from the National Climate Data Center (www.ncdc.noaa.gov), which were measured at a station located in the Beijing Capital International Airport.

Comment NO.11: *Is all the data in this paper daily data? Please give make it clear in the paper.*

Response:

Yes, all the data used in this manuscript are daily averages and this has been clarified in the method section of the revised manuscript (Page 4 line105).

To be more specific, daily PM_{2.5} filter samples were collected for 23.5 h, from 9:30 am to 9:00 am the next day; thus, PM_{2.5} and its components were daily averaged data. Gaseous pollutants (SO₂, O₃, NO_x, etc.), RH and temperature with a time resolution of mins were averaged according to the filter sampling time period. Daily solar radiation data was used as it is.

Comment NO.12: *SOR is the conversion ratio of SO₂, I doubt whether it can indicate the conversion rate (or speed) as you mentioned in your paper (e.g. Page 1, line 21, Page 10, line 14 etc.) What is the relationship of O₃ and atmospheric oxidative capacity? AWC and RH? Please reconsider in your statement and discussions? (Page 8, line 10, Page 9, line 10-11 etc.).*

Response:

- 1) We agree with the referee that SOR is defined as the ratio of sulfate to total sulfur and it is not the SO₂-sulfate conversion rate. However, due to the long chemical lifetime of sulfate, sulfate tends to accumulate with chemical production within at least 24 hrs, which could be best reflected in SOR, the ratio of sulfate to total sulfur. SOR has been widely used as an indicator of SO₂-to-sulfate conversion in numbers of references (Sun et al., 2014; Zheng et al., 2015), where a high SOR reflects a high SO₂-to-sulfate conversion rate on average during the measurement period.
- 2) Atmospheric oxidative capacity relates to the concentrations of major oxidants such as OH radicals, O₃, etc. (Murray et al., 2009). Since O₃ is a major oxidant and a precursor to other major oxidants, including OH radicals, to a certain degree, O₃ can be used as a proxy for atmospheric oxidative capacity. To improve clarity, atmospheric oxidative capacity was replaced by the appropriate oxidant in each context in the revised manuscript.
- 3) The AWC calculated using the ISORROPIA-II thermodynamic model (<http://isorro피아.eas.gatech.edu>). Please also refer to the revised SI (Page 35 lines 661–663). In brief, AWC is a function of aerosol mass concentration, aerosol chemical composition, RH, etc.

Changes in Manuscript: Atmospheric oxidative capacity was replaced by the appropriate oxidants. Please refer to the revised manuscript, Page 7 line 197, Page 11 line 291, Page 12 lines 323 and 342.

Comment NO.13: *The fitting methods were used in this paper (Fig. 5 and Fig. S5), please give the evaluation parameters (such as p-value and R) of the fitting method to prove the validity and accuracy of the fitting. Also in Fig 5b, the last 2 box bins only have 1-2 points, does the results make sense?*

Response: Accepted

- 1) R² has been added to Fig. 5 in the revised manuscript (Page 25).
- 2) In Fig. 5 (Page 25 in the revised manuscript), O₃ concentrations were grouped by 5 ppb intervals and RH by 5 % intervals. There were only a few data points on the right-hand sides of these figures because there were only a few days with daily average O₃ (RH) above 70 ppb (70 %). However, the shapes of the fits are not much different when we group them by the number of data points in each bin, as shown in Fig. R6 in this response. O₃ in Fig. R6a was the original method that grouped by 5 ppb intervals, while O₃ in Fig. R6b were grouped with an approximately equal number of data points (15–16) in each bin, which shows the robustness of our fitting.

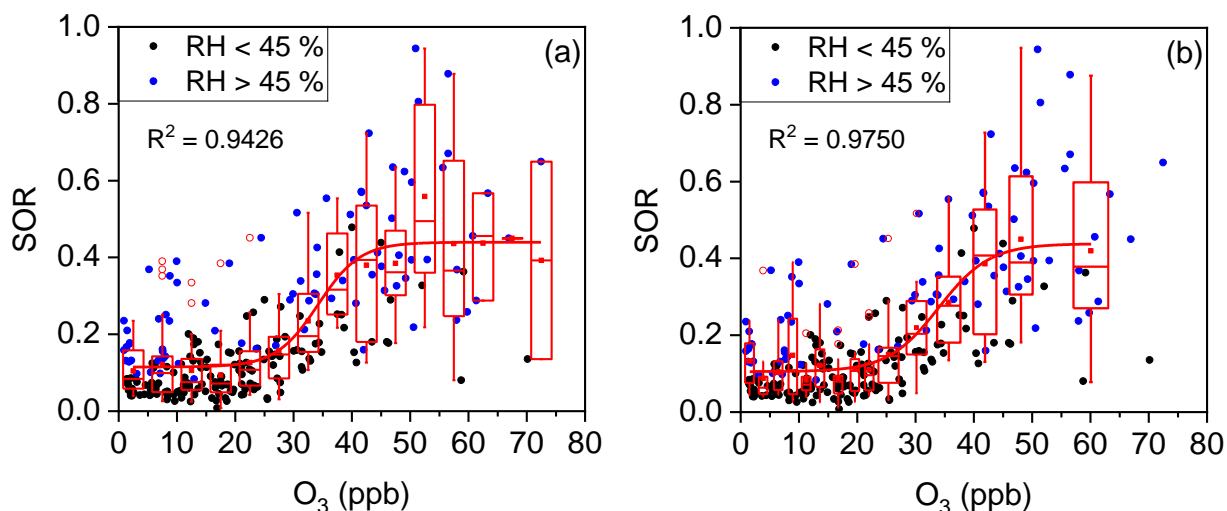


Figure R6. Plots of the SOR against O₃, grouped by RH. The solid blue circles represent RH > 45 % and the solid black circles represent RH < 45 %. The boxes represent, from top to bottom, the 75th, 50th, and 25th percentiles in each bin ((a) $\Delta O_3 = 5$ ppb, (b) variable ΔO_3 , 15–16 data points in each bin). The whiskers, solid red squares, and open red circles represent 1.5 times IQR, mean values, and outlier data points, respectively. The red lines are best fits to the mean values based on a sigmoid function. Data for days with rain or snow were excluded from these plots.

Changes in Manuscript: R^2 has been added to the plots that containing fitting lines. Please refer to the revised manuscript, Page 25 Fig. 5, Page 26 Fig. 6, Page 27 Fig. 7. Please also refer to the revised SI, Page 37 Fig. S3, and Page 40 Fig. S7.

Comment NO.14: Give the right form of the author's name in Page 1 and Page 12. There should be a space between units and the quantity.

Response: Accepted.

Changes in Manuscript:

- 1) The right form of the author's name has been given. Please refer to the revised manuscript, Page 1 line 2.
- 2) Space has been added between number and % or number between °C. Please refer to the revised manuscript, Page 1 line 15, Page 4 lines 111 and 112, Page 5 line 139, Page 6 lines 147, 157, 159, 166, and 168, Page 7 lines 171 and 173, Page 8 lines 211 and 216, Page 9 line 235, Page 10 lines 279, 281, and 288, Page 11 line 299, Page 12 line 332, Page 25 lines 579 and 580, Page 26 line 586, Page 27 lines 590 and 591, Page 29 line 602, and Page 31 line 613.

References

Berglen, T. F., Berntsen, T. K., Isaksen, I. S. A., and Sundet, J. K.: A global model of the coupled

- sulfur/oxidant chemistry in the troposphere: The sulfur cycle, *J. Geophys. Res. Atmos.*, 109, <https://doi.org/10.1029/2003jd003948>, 2004.
- Brothers, L. A., Dominguez, G., Abramian, A., Corbin, A., Bluen, B., and Thiemens, M. H.: Optimized low-level liquid scintillation spectroscopy of S-35 for atmospheric and biogeochemical chemistry applications, *Proc. Natl. Acad. Sci. U.S.A.*, 107, 5311-5316, <https://doi.org/10.1073/pnas.0901168107>, 2010.
- Ding, J., Zhao, P., Su, J., Dong, Q., Du, X., and Zhang, Y.: Aerosol pH and its driving factors in Beijing, *Atmos. Chem. Phys.*, 19, 7939-7954, <https://doi.org/10.5194/acp-19-7939-2019>, 2019.
- Finlayson-Pitts, B. J., and Pitts, J. N. Jr.: *Chemistry of the upper and lower atmosphere: Theory, experiments, and applications*, Academic Press, San Diego, California, 2000.
- Fu, A.: Study on peroxide concentration and its influence factors in the urban atmosphere, Master, College of Environmental and Resource Sciences, Zhejiang University, Hangzhou, China, 2014 (in Chinese).
- He, P., Alexander, B., Geng, L., Chi, X., Fan, S., Zhan, H., Kang, H., Zheng, G., Cheng, Y., Su, H., Liu, C., and Xie, Z.: Isotopic constraints on heterogeneous sulfate production in Beijing haze, *Atmos. Chem. Phys.*, 18, 5515-5528, <https://doi.org/10.5194/acp-18-5515-2018>, 2018.
- Lang, J. L., Cheng, S. Y., Li, J. B., Chen, D. S., Zhou, Y., Wei, X., Han, L. H., and Wang, H. Y.: A Monitoring and modeling study to investigate regional transport and characteristics of PM_{2.5} pollution, *Aerosol Air Qual. Res.*, 13, 943-956, <https://doi.org/10.4209/aaqr.2012.09.0242>, 2013.
- Li, Y. R., Ye, C. X., Liu, J., Zhu, Y., Wang, J. X., Tan, Z. Q., Lin, W. L., Zeng, L. M., and Zhu, T.: Observation of regional air pollutant transport between the megacity Beijing and the North China Plain, *Atmos. Chem. Phys.*, 16, 14265-14283, <https://doi.org/10.5194/acp-16-14265-2016>, 2016.
- Liu, M., Song, Y., Zhou, T., Xu, Z., Yan, C., Zheng, M., Wu, Z., Hu, M., Wu, Y., and Zhu, T.: Fine particle pH during severe haze episodes in northern China, *Geophys. Res. Lett.*, 44, 5213-5221, <https://doi.org/10.1002/2017GL073210>, 2017a.
- Liu, X., Sun, K., Qu, Y., Hu, M., Sun, Y., Zhang, F., and Zhang, Y.: Secondary formation of sulfate and nitrate during a haze episode in megacity Beijing, China, *Aerosol Air Qual. Res.*, 2246 - 2257, <https://doi.org/10.4209/aaqr.2014.12.0321>, 2015.
- Liu, Y. C., Wu, Z. J., Wang, Y., Xiao, Y., Gu, F. T., Zheng, J., Tan, T. Y., Shang, D. J., Wu, Y. S., Zeng, L. M., Hu, M., Bateman, A. P., and Martin, S. T.: Submicrometer particles are in the liquid state during heavy haze episodes in the urban atmosphere of Beijing, China, *Environ. Sci. Technol. Lett.*, 4, 427-

432, <https://doi.org/10.1021/acs.estlett.7b00352>, 2017b.

Liu, Y. J., Zhu, T., Zhao, D. F., and Zhang, Z. F.: Investigation of the hygroscopic properties of $\text{Ca}(\text{NO}_3)_2$ and internally mixed $\text{Ca}(\text{NO}_3)_2/\text{CaCO}_3$ particles by micro-Raman spectrometry, *Atmos. Chem. Phys.*, 8, 7205-7215, <https://doi.org/10.5194/acp-8-7205-2008>, 2008.

Murray, L. T., Mickley, L., Kaplan, J. O., Sofen, E. D., Alexander, B., Jones, D. B., and Jacob, D. J.: Evolution of the oxidative capacity of the troposphere since the Last Glacial Maximum, 3589-3622, <https://doi.org/10.5194/acp-14-3589-2014>, 2009.

Sun, Y. L., Jiang, Q., Wang, Z. F., Fu, P. Q., Li, J., Yang, T., and Yin, Y.: Investigation of the sources and evolution processes of severe haze pollution in Beijing in January 2013, *J. Geophys. Res. Atmos.*, 119, 4380-4398, <https://doi.org/10.1002/2014JD021641>, 2014.

Wang, R., Xu, X., Jia, S., Ma, R., Ran, L., Deng, Z., Lin, W., Wang, Y., and Ma, Z.: Lower tropospheric distributions of O_3 and aerosol over Raoyang, a rural site in the North China Plain, *Atmos. Chem. Phys.*, 17, 3891-3903, <https://doi.org/10.5194/acp-17-3891-2017>, 2017.

Xu, L., Duan, F., He, K., Ma, Y., Zhu, L., Zheng, Y., Huang, T., Kimoto, T., Ma, T., Li, H., Ye, S., Yang, S., Sun, Z., and Xu, B.: Characteristics of the secondary water-soluble ions in a typical autumn haze in Beijing, *Environ. Pollut.*, 227, 296-305, <https://doi.org/10.1016/j.envpol.2017.04.076>, 2017.

Yang, Y. R., Liu, X. G., Qu, Y., An, J. L., Jiang, R., Zhang, Y. H., Sun, Y. L., Wu, Z. J., Zhang, F., Xu, W. Q., and Ma, Q. X.: Characteristics and formation mechanism of continuous hazes in China: a case study during the autumn of 2014 in the North China Plain, *Atmos. Chem. Phys.*, 15, 8165-8178, <https://doi.org/10.5194/acp-15-8165-2015>, 2015.

Ye, C., Liu, P., Ma, Z., Xue, C., Zhang, C., Zhang, Y., Liu, J., Liu, C., Sun, X., and Mu, Y.: High H_2O_2 concentrations observed during haze periods in wintertime of Beijing: Importance of H_2O_2 -oxidation in sulfate formation, *Environ. Sci. Technol. Lett.*, <https://doi.org/10.1021/acs.estlett.8b00579>, 2018.

Zheng, G. J., Duan, F. K., Su, H., Ma, Y. L., Cheng, Y., Zheng, B., Zhang, Q., Huang, T., Kimoto, T., Chang, D., Poschl, U., Cheng, Y. F., and He, K. B.: Exploring the severe winter haze in Beijing: the impact of synoptic weather, regional transport and heterogeneous reactions, *Atmos. Chem. Phys.*, 15, 2969-2983, <https://doi.org/10.5194/acp-15-2969-2015>, 2015.

RH and O₃ concentration as two prerequisites for sulfate formation

Yanhua Fang^{1#} and Chunxiang Ye^{1#}, Junxia Wang¹, Yusheng Wu¹, Min Hu¹, Weili Lin², Fanfan Xu¹,
Tong Zhu^{1*}

¹BIC-ESAT and SKL-ESPC, College of Environmental Sciences and Engineering, Peking University, Beijing, 100871, China

²College of Life and Environmental Sciences, Minzu University of China, Beijing 100081, China

[#]These authors contributed equally to the paper.

*Correspondence to: Tong Zhu (tzhu@pku.edu.cn)

Abstract. Sulfate formation mechanisms have been discussed extensively but are still disputed. In this work, a year-long particulate matter (PM_{2.5}) sampling campaign was conducted together with measurements of gaseous pollutant concentrations and meteorological parameters in Beijing, China, from March 2012 to February 2013. The sulfur oxidation ratio (SOR), an indicator of secondary sulfate formation, displayed a clear summer peak and winter valley, even though no obvious seasonal variations in sulfate mass concentration were observed. A rapid rise in the SOR was found at a RH threshold of ~45 % or an O₃ concentration threshold of ~35 ppb, allowing us to first introduce the idea that RH and O₃ concentrations are two prerequisites for rapid sulfate formation via multiphase reactions. In the case of the RH threshold, this is consistent with current understanding of the multiphase formation of sulfate, since it relates to the semisolid-to-liquid phase transition of atmospheric aerosols. Correlation analysis between SOR and AWC further backed this up. In the case of the O₃ concentration threshold, this is consistent with the consumption of liquid oxidants in multiphase sulfate formation. The thresholds introduced here lead us to better understanding of the sulfate formation mechanism and sulfate formation variations. H₂O₂ might be the major oxidant of sulfate formation, since another liquid phase oxidant, O₃, has previously been shown to be unimportant. The seasonal variations in sulfate formation could be accounted for by variations in the RH and O₃ prerequisites. For example, over the year-long study, the fastest SO₂-to-sulfate conversion occurred in summer, which was associated with the highest values of O₃ (and also H₂O₂) concentration and RH. The SOR also displayed variations with pollution levels, i.e., the SOR increased with PM_{2.5} in all seasons. Such variations were primarily associated with a transition from the slow gas phase formation of sulfate to rapid multiphase reactions, since RH increased higher than its prerequisite value of around 45% as pollution evolved. In addition, the self-catalytic nature of sulfate formation (i.e., the formation of hydrophilic sulfate aerosols under high RH conditions results in

31 an increase in aerosol water content, which results in greater particle volume for further multiphase sulfate
32 formation) also contributed to variations among the pollution scenarios.

33 **1 Introduction**

34 Beijing, the capital of China, suffers from serious air pollution due to its rapid economic growth and
35 urbanisation (Hu et al., 2015). The chemical composition and sources of fine particulate matter (PM_{2.5})
36 in Beijing have been studied extensively (Han et al., 2015; Lv et al., 2016; Zhang et al., 2013; Zheng et
37 al., 2005). Secondary components, especially sulfate, nitrate, and ammonium (SNA), are the main
38 contributors to PM_{2.5} (Huang et al., 2014a). On the most severely polluted days, SNA account for more
39 than half of total PM_{2.5} mass concentrations and play a more important role than on clean days (Quan et
40 al., 2014; Wang et al., 2014b; Zheng et al., 2015b).

41 The kinetics and mechanisms of the formation of sulfate, a major component of SNA, are complex and
42 remain unclear (Ervens, 2015; Harris et al., 2013; Warneck, 2018). For example, two key questions
43 concerning sulfate formation are: (1) exactly how do various parameters (oxidants, catalysts,
44 meteorological conditions, etc.) influence sulfate formation, and (2) how do multiple formation routes
45 compete and contribute together to sulfate formation under ambient conditions. In general, sulfate is
46 produced from SO₂ via gas phase oxidation reactions involving the hydroxide radical (OH) and Criegee
47 intermediates (Gleason et al., 1987; Sarwar et al., 2014; Vereecken et al., 2012), heterogeneous reactions
48 (mainly on dust aerosols), and multiphase transformations with O₃, H₂O₂, or O₂ (catalysed by transition
49 metal ions (TMIs) (i.e., TMIs + O₂) and NO₂ (NO₂ + O₂)) as liquid phase oxidants, which occur mainly
50 in clouds but also in aerosol droplets near the ground (Zhu et al., 2011).

51 Due to the major role of multiphase transformations, sulfate production is presumed to be self-catalysed,
52 i.e., the formation of hydrophilic sulfate aerosols under high relative humidity (RH) conditions results in
53 an increase in aerosol water content (AWC), which results in greater particle volume for further
54 multiphase sulfate formation (Cheng et al., 2016; Pan et al., 2009; Xu et al., 2017). Analyses of the
55 correlation of sulfate formation with RH and AWC have been conducted to test this hypothesis, using the
56 concept of the sulfur oxidation ratio (SOR), defined as the molar ratio of sulfate to total sulfur (= sulfate
57 + SO₂). It is used to indicate the magnitude of the secondary formation of sulfate and expressed as (Wang
58 et al., 2005):

59
$$\text{SOR} = \frac{n_{\text{SO}_4^{2-}}}{n_{\text{SO}_4^{2-}} + n_{\text{SO}_2}}, \quad (\text{Eq. 1})$$

60 where $n_{\text{SO}_4^{2-}}$ and n_{SO_2} represent the molar concentrations of sulfate and SO_2 , respectively. Even though
61 regional transport or intrusion of SO_2 or sulfate (or local sulfate emissions) would modify the SOR, it has
62 still often been a relatively good proxy of secondary sulfate formation (i.e., local SO_2 -to-sulfate
63 conversion). For example, Sun et al. (2014; 2013) found positive correlations between the SOR and RH,
64 and observed rapid increases in SORs at elevated RH levels. Xu et al. (2017) found positive correlations
65 of the SOR with both RH and AWC. Multiphase transformation routes, including O_3 oxidation, TMI +
66 O_2 , and $\text{NO}_2 + \text{O}_2$, are pH-sensitive and suppressed at low pH (Seinfeld and Pandis, 2006). Sulfate
67 production raises the acidity of aerosols and therefore the multiphase transformations of sulfate are
68 presumed to be self-constrained (Cheng et al., 2016). For example, a significant contribution from the O_3
69 oxidation route can only be expected under alkaline conditions (e.g., sea-salt), otherwise, O_3 oxidation is
70 a minor pathway for sulfate formation (Alexander et al., 2005; Sievering et al., 2004). How the self-
71 constraining nature of sulfate formation influences the relative significance of the TMI + O_2 and $\text{NO}_2 +$
72 O_2 routes is still under debate. Cheng et al. (2016) proposed that the $\text{NO}_2 + \text{O}_2$ route is important during
73 severe haze events under neutral pH conditions (He et al., 2018; Wang et al., 2016). Guo et al. (2017)
74 suggested that aerosols are acidic in Beijing (except for during the limited cases of dust or sea-salt events),
75 casting doubt on the importance of the $\text{NO}_2 + \text{O}_2$ route in sulfate formation (Liu et al., 2017a). According
76 to laboratory-based Raman spectroscopy studies, sulfate can be produced via the aqueous oxidation of
77 SO_2 by $\text{NO}_2 + \text{O}_2$, with an SO_2 reactive uptake coefficient of 10^{-5} , which represents an atmospherically
78 relevant value (Yu et al., 2018), whereas others have suggested that this route is of minor importance in
79 the atmosphere (Li et al., 2018; Zhao et al., 2018). In addition, Xie et al. (2015) proposed that NO_2 could
80 enhance the formation of sulfate in certain cases, for example, in biomass burning plumes or dust storms
81 (He et al., 2014). Evaluation of the contribution of TMI + O_2 reactions appears to be more complex since
82 it depends on aerosol acidity, solubility, oxidation state, and the synergistic effects of different TMI
83 (Deguillaume et al., 2005; Warneck, 2018).

84 The compensating effects among AWC, aerosol acidity, and the concentrations of precursors and catalysts
85 show that the kinetics and mechanisms of sulfate formation are highly complex. It can be inferred that
86 there is competition between the various routes, with dependences on atmospheric conditions (e.g.,
87 seasonal and pollution level variations) likely, but this has not received much research attention previously.

88 Here, daily PM_{2.5} samples were collected in Beijing from March 2012 to February 2013 and their chemical
89 composition was analysed. The main parameters that influenced sulfate formation (i.e., RH, O₃
90 concentration, TMIs, etc.) were determined. This valuable dataset enabled us to explore: (1) the specific
91 role of each influencing factor in sulfate formation, and (2) how multiple sulfate formation routes compete
92 in different seasons and under various pollution scenarios.

93 **2 Measurements and methodology**

94 **2.1 Measurements**

95 **2.1.1 Measurement stations**

96 The two measurement stations are shown in Fig. 1. The PKU station (116.30 °E, 39.99 °N) is about 20 m
97 above ground level at the campus of Peking University, Beijing, China (Liang et al., 2017). Daily PM_{2.5}
98 samples were collected using a four-channel sampler (TH-16A; Wuhan Tianhong Instruments, China) at
99 a flow rate of 16.7 L min⁻¹ from 1 March 2012 to 28 February 2013. The gaseous pollutants SO₂, NO_x,
100 and O₃ were measured with a pulsed fluorescence SO₂ analyser (Model 43i TLE; Thermo Fisher Scientific,
101 Waltham, MA, USA), chemiluminescence NO–NO₂–NO_x analyser (Model 42i TL; Thermo Fisher
102 Scientific), and an ultraviolet photometric O₃ analyser (Model 49i; Thermo Fisher Scientific), respectively.
103 Temperature and RH were also monitored (MSO; Met One Instruments, Grants Pass, OR, USA). Solar
104 radiation data were obtained from the Beijing Meteorological Observatory Station (116.47 °E, 39.81 °N).
105 Daily averages were used for all analysis conducted in this work.

106 **2.1.2 Filter sampling and analysis**

107 Each PM_{2.5} sample set consisted of one quartz filter (47 mm; Whatman QM/A, Maidstone, England) and
108 three Teflon filters (47 mm; pore size = 2 μm; Whatman PTFE). The quartz filters were baked for 5.5 h
109 at 550 °C before use. The Teflon filters were weighed in a weighing room before and after sampling using
110 a delta range balance (0.01 mg/0.1 mg precision; AX105; Mettler Toledo, Switzerland). To minimise
111 contamination, all Teflon filters were placed in a super clean room (temperature = 22 ± 1 °C; RH = 40 ±
112 2 %) for 24 h before being weighed. After sampling, all filters were stored at –20 °C prior to analysis.
113 Water soluble cations (Na⁺, NH₄⁺, K⁺, Mg²⁺, and Ca²⁺) and anions (SO₄²⁻, NO₃⁻, Cl⁻, and F⁻) were
114 measured using ion chromatography (ICS-2500 and ICS-2000; DIONEX, USA). Trace elements (Na, Mg,
115 Al, Ca, Ti, Cr, Mn, Fe, Co, Ni, Cu, Zn, Se, Mo, Cd, Ba, Tl, Pb, Th, and U) were analysed by inductively

116 coupled plasma–mass spectrometry (ICP–MS, X-Series; Thermo Fisher Scientific). Organic carbon (OC)
117 and elemental carbon (EC) were measured using a thermal/optical carbon analyser (RT-4; Sunset
118 Laboratory Inc., Tigard, OR, USA). The procedure for the measurement of water soluble Fe has been
119 described in detail in a previous study (Xu et al., 2018).

120 **2.2 Estimation of the mass concentrations of PM_{2.5} components**

121 The chemical components of PM_{2.5} were divided into eight categories: sulfate, nitrate, ammonium,
122 organic matter (OM), EC, minerals, trace element oxides (TEOs), and others. The mass concentrations of
123 OM, minerals, and TEOs were calculated from OC, Al, and trace element concentrations, respectively.
124 The details of this method are provided in the supplementary information (SI). For minerals, validation
125 of the method using only Al to represent all minerals is shown in Fig. S1. TEOs mostly originated from
126 anthropogenic sources (Fig. S2).

127 **2.3 Quality assurance and quality control**

128 The PM_{2.5} sampling instruments were cleaned and calibrated every 2–3 months. Before the daily filter
129 replacement, filter plates were scrubbed with degreasing cotton that had been immersed in
130 dichloromethane. For water soluble ions, OC/EC, and trace element measurements, standard solutions
131 were analysed before each series of measurements. The R^2 values of the calibration curves were all >
132 0.999. For water soluble ion measurements, beakers, tweezers, and vials were cleaned with deionised
133 water (18.2 MΩ; Milli-Q, USA) three times before use. Certified reference standards (National Institute
134 of Metrology, China) were used for calibration. For OC/EC measurements, tweezers and scissors were
135 scrubbed with degreasing cotton immersed in dichloromethane for every filter. Total organic carbon
136 (TOC) was calculated based on calibration with external standard solutions. For trace element
137 measurements, containers and tweezers were cleaned three times with nitric acid before use, and the
138 analysis of a certified reference standard (NIST SRM-2783) was used to verify accuracy. The recovery
139 of all measured trace elements fell within ± 20 % of their certified values. For gaseous pollutants and
140 meteorological parameters, all instruments were maintained and calibrated weekly based on
141 manufacturers' protocols.

142 **3 Results and discussion**

143 **3.1 General description**

144 The annual and seasonal mean (\pm one standard deviation (SD)) concentrations of PM_{2.5} and its seven
145 major **known** components are summarised in Table 1. The annual mean PM_{2.5} concentration was 84.1 (\pm
146 63.1) $\mu\text{g m}^{-3}$, which is more than two times greater than the Chinese National Ambient Air Standard
147 **annual mean concentration** of 35 $\mu\text{g m}^{-3}$. On 145 of the 318 (46 %) measurement days, daily mean PM_{2.5}
148 concentrations were above the Chinese National Ambient Air Standard 24 h mean concentration of 75 μg
149 m^{-3} . Time series of PM_{2.5} concentrations and its seven major **known** components are shown in Fig. 2.
150 Seasonal variations in PM_{2.5} loading are obvious, with spring and winter peaks and summer and autumn
151 valleys. OM and EC concentrations **displayed** common seasonal variations, with a plateau from mid-
152 October to mid-February and a valley in summer (Fig. 2), which resembles the variations in PM_{2.5}, K⁺,
153 **Cl⁻, and F⁻ (Figs. 2 and 3). The seasonal variations in minerals also indicate an important contribution of**
154 **dust events to PM_{2.5} loading during spring, which is a well-known phenomenon (Zhang et al., 2003;**
155 **Zhuang et al., 2001). TEOs displayed no obvious seasonal variations (Fig. 2). SNA accounted for more**
156 **than one-third of PM_{2.5} annually and showed similar seasonal variations to that of PM_{2.5} (Fig. 2), with the**
157 **notable exception that sulfate became the highest contributor to PM_{2.5} (~25 %) in summer (Fig. 4). The**
158 **summer peak in sulfate could be accounted for by fast secondary formation, as will be discussed later.**
159 **On an annual basis, the seven major known components accounted for over 80 % of PM_{2.5} (Fig. 4). The**
160 **diversity of the seasonal variations in PM_{2.5} and its major components found in our study imply that there**
161 **were seasonal variations in both the primary sources and secondary formation of PM_{2.5}.**

162 **3.2 Influence of various parameters on sulfate formation**

163 To further explore the parameters that influenced sulfate formation, SORs were plotted against RH and
164 the concentrations of O₃, NO₂, and Fe (total Fe, including both water soluble and water insoluble Fe),
165 which is a major tracer of transition metals (Figs. 5 and 6).

166 As shown in Fig. 5a, an RH threshold of ~45 % was critical for efficient SO₂ oxidation (i.e., a
167 high SOR). Such a threshold effect was thought to be reasonable given that AWC increases sharply **when**
168 **RH was above a threshold of 45 %**, at which the aerosol undergoes a phase transition from a (semi-)solid
169 particle to a droplet (Pan et al., 2009; Russell and Ming, 2002). **Further correlation analysis between SOR**
170 **and AWC further supports that the multiphase reactions are responsible for sulfate formation. (Fig. S3).**

171 Our observation of a daily average RH threshold of ~45 % is in line with previous reports of 40–50 %
172 (Liu et al., 2015; Quan et al., 2015; Xu et al., 2017; Yang et al., 2015; Zheng et al., 2015b), but is slightly
173 lower than the *in situ* phase transition threshold RH of 50–60 % previously observed in Beijing (Liu et
174 al., 2017b). Correlation analysis of SOR and RH (or AWC) has often been conducted in previous studies.
175 For example, Wang et al. (2005) found a weak positive correlation of SORs with RH ($R = 0.38$), while
176 Sun et al. (2006) found a strong positive correlation ($R = 0.96$). However, the analysis in the present work
177 and those of a few previous studies revealed that the relationship between the SOR and RH is nonlinear
178 (Sun et al., 2013; Sun et al., 2014; Zheng et al., 2015b). In fact, the RH threshold suggests that high RH
179 (or AWC) is a prerequisite for fast sulfate formation via multiphase reactions, which are known to account
180 for the majority of sulfate accumulation.

181 From the large scattering of data points around the fit line in Fig. 5a, it might be inferred that RH
182 was not the only prerequisite for fast SO₂-to-sulfate conversion. As shown in Fig. 5b, a significant increase
183 in the SOR was also observed at an O₃ concentration threshold of ~35 ppb. High O₃ concentrations (i.e., >
184 35 ppb) were accompanied by high SOR values of ~0.4 (right-hand side of Fig. 5b). Correlation analyses
185 of SORs with O₃ have been conducted but inconsistent results were reported. Wang et al. (2005) found a
186 weak positive correlation between SORs and O₃ ($R = 0.47$) for continuous observations in Beijing during
187 2001–2003. However, Liu et al. (2015) found a weak negative correlation between SORs and O₃ ($R =$
188 -0.53 , $p = 0.01$) during a haze episode in September 2011. Zhang et al. (2018) found no correlation
189 between SORs and O₃ during winter haze days in 2015. Quan et al. (2015) found that the SOR decreased
190 with O₃ when O₃ concentrations were lower than 15 ppb, but increased with O₃ when O₃ concentrations
191 were higher than 15 ppb, for observations made during autumn and winter 2012. In the present study, our
192 observations revealed that the relationship between the SOR and O₃ concentration, like RH, was nonlinear
193 and that a high O₃ concentration was another prerequisite for fast sulfate formation. Such a conclusion
194 was a surprise first, since O₃ oxidation was not thought to be a major route for SO₂-to-sulfate conversion
195 (He et al., 2018; Sievering et al., 2004). However, as a primary precursor to OH radicals and H₂O₂ (via
196 HO₂), (Lelieveld et al., 2016; Lu et al., 2017), high O₃ concentrations (e.g., > 35 ppb) correspond to a
197 high concentration of oxidants, which favors multiphase sulfate formation and thus a high SOR, whereas
198 low O₃ concentrations suggest a lack of available oxidants for multiphase SO₂-to-sulfate conversion and
199 thus a low SOR. In addition, the simultaneous occurrence of low SORs and low O₃ concentrations had a
200 secondary cause. Low O₃ concentrations in the Beijing urban area were often due to the titration of O₃ by

201 NO (Li et al., 2016), which accumulated together with SO₂ (Fig. S4). The accumulation of SO₂, which
202 “diluted” the SOR (Eq. 1), was thus naturally accompanied by the titration of O₃. The L-shaped
203 dependence of the SOR on several other primary pollutants, such as EC, NO, and Se (Fig. S5), further
204 confirmed this secondary cause. Therefore, the accumulation of primary pollutants might also help to
205 explain the low SOR values of ~0.1 on the left-hand side of Fig. 5b, in addition to the lack of available
206 oxidants for multiphase SO₂-to-sulfate conversion.

207 The large scattering of data points around the fit line in Fig. 5b suggests that O₃ concentration,
208 like RH, was not the only prerequisite for fast SO₂-to-sulfate conversion. The dependence of the SOR on
209 RH was separated into low (< 35 ppb) and high (> 35 ppb) O₃ groups (solid black circles and solid blue
210 circles, respectively, in Fig. 5a). SOR values above the fit line are found mostly for the high O₃ group.
211 After the dependence of the SOR on O₃ concentration was separated into low (< 45 %) and high (> 45 %)
212 RH groups (solid black circles and solid blue circles, respectively, in Fig. 5b), a similar pattern was found
213 for the high RH group. In other words, fast multiphase SO₂-to-sulfate conversion could only occur when
214 both O₃ and RH exceeded their respective thresholds simultaneously.

215 The seasonal variation of such thresholds of RH and O₃ were further discussed. As shown in Fig.
216 6, RH threshold was roughly around 45 % during all four seasons in Beijing. While the threshold of O₃
217 varied among seasons (Fig.7). A turning point of 25–40 ppb was observed for fast SOR increase in spring,
218 summer and autumn, while the turning point is not clear due to lack of high O₃ data in winter. The
219 variation of O₃ threshold value might be due to the shifts of O₃-H₂O₂ relationship which might be modified
220 by temperature etc. in different seasons. Despite of the variation of thresholds of RH and O₃ in different
221 seasons or even in different sampling location (not discussed here), the thresholds of RH and O₃ for fast
222 sulfate formation further found in our study has its implications on sulfate formation mechanism (see
223 below).

224 The SORs was further plot against Fe and NO₂. No clear dependence of the SOR on concentrations
225 of Fe or NO₂ was found (Figs. 8a and 8b). Possible reasons and implications of this result will be discussed
226 in the following section.

227 3.3 Implications for sulfate formation mechanisms

228 Our observations of the factors that influence sulfate formation have implications for sulfate formation
229 routes and its variations among seasons and pollution conditions.

230 In retrospect, thresholds in RH and O₃ concentrations were found to be critical to the SOR,
231 suggesting that AWC and liquid phase oxidant were two prerequisites for fast multiphase SO₂-to-sulfate
232 conversion. H₂O₂ and O₃ are the two liquid phase oxidants which are responsible for sulfate formation.
233 The O₃ oxidation route was proposed not important in high aerosol acidity areas, such as Beijing (Guo et
234 al., 2017; Sievering et al., 2004). A recent study on aerosol pH in Beijing showed that the PM_{2.5} was
235 acidic (RH > 30 %) (Ding et al., 2019), confirming a minor contribution from O₃ oxidation. H₂O₂ was
236 then the only possible oxidant responsible for sulfate formation. Although direct measurements of
237 aqueous H₂O₂ were not performed in this study, the H₂O₂ concentrations in Beijing reported by Fu (2014)
238 were found to be positively correlated with temperature. By assuming the reported H₂O₂-Temperature
239 relationship applicable to our measurements, a proxy H₂O₂ concentration was then estimated. As shown
240 in Fig. S6, maximum concentration of H₂O₂ in summer is expected and confirmed, which is in line with
241 the fastest sulfate formation in summer all over the measurement year. SOR was further plotted against
242 H₂O₂ and positive correlation was found between them (Fig. S7). In addition, coincident increases in the
243 concentration of H₂O₂ and PM_{2.5} in winter of Beijing also lead to an important role of the H₂O₂ oxidation
244 route in sulfate formation (Ye et al., 2018). Based on the above discussions, we propose that H₂O₂ might
245 be the major oxidant for sulfate formation in Beijing.

246 The plot of SORs against Fe, the dominant transition metal species, shows no clear dependence
247 (Figs. 8a and S8). Similarly, the plot of SORs against NO₂ shows no clear dependence either (Fig. 8b). If
248 Fe acted as a catalyst and thus its concentration might not be directly proportional to SORs. Therefore,
249 such a pattern does not safely exclude TMI_s + O₂ as a major route for sulfate formation. Several laboratory
250 studies excluded NO₂ as a direct oxidant in SO₂-to-sulfate conversion. For example, Zhao et al. (2018)
251 tested the oxidation of SO₂ by NO₂ in an N₂ atmosphere and concluded that NO₂ is not an important
252 oxidant, since NO₂ was more likely to undergo disproportionation (Li et al., 2018). However, Yu et al.
253 (2018) further explored this reaction, and found that the reaction rate was 2–3 orders of magnitude greater
254 in an O₂ + N₂ atmosphere, indicating potentially important roles of NO₂ + O₂ oxidation in sulfate
255 formation (He et al., 2014; Ma et al., 2018). As with Fe, if NO₂ acted as a catalyst, its concentration might
256 not be directly proportional to that of sulfate. Therefore, such a pattern does not safely exclude NO₂ + O₂
257 as a major route for sulfate formation either. Although direct aerosol pH measurement is not available
258 here, previous studies has reported a mean aerosol pH value of 4.2 with a low limit of 3.0 in Beijing (Ding
259 et al., 2019; Liu et al., 2017), which suggests that several routes of sulfate formation, including NO₂ + O₂,

260 TMI_s + O₂, O₃ oxidation etc., are suppressed. Hence, we carefully propose here neither TMI_s +O₂ nor
261 NO₂+O₂ seem to be a major route for sulfate formation.

262 On one hand, a direct measurement of aerosol pH is also urgently needed in the future to examine
263 our proposal here; on another hand, our proposal here has further implication on the understanding of
264 sulfate formation. Previously, aerosol surface area and concentrations of Fe, Mn, and NO₂ were used in
265 model evaluations of catalytic sulfate formation in the boundary layer (Wang et al., 2014a; Zheng et al.,
266 2015a). However, our proposals here suggest that a careful reassessment of such calculations is required.
267 In addition, model calculations have often suggested important contributions of in-cloud processes to
268 sulfate accumulation near the ground (Barth et al., 2000), although few observational constraints are
269 available for confirmation of these model results (Harris et al., 2014; Shen et al., 2012). The O₃
270 concentration and RH prerequisites found in the present work might indicate a major role of *in situ* sulfate
271 formation in the boundary layer, via multiphase reactions with H₂O₂ as the main oxidant, rather than in-
272 cloud processes and intrusion from the free troposphere.

273 As the two prerequisites showed strong seasonal and pollution level variations over the
274 measurement year, the SOR exhibited corresponding variations. As shown in Fig. 9, SORs displayed clear
275 seasonal variations, with the highest value (± 1 SD) of 0.46 (± 0.22) in summer, followed by spring (0.23
276 ± 0.14), autumn (0.18 ± 0.15), and winter (0.09 ± 0.05). The highest SOR (i.e., fastest SO₂-to-sulfate
277 conversion rate) was found in summer, which is not surprising because the ambient conditions in summer
278 were conducive SO₂-to-sulfate conversion (Wang et al., 2005). RH and O₃ concentrations in summer were
279 not only the highest in the year, but on average were also both higher than their thresholds of 45 % and
280 35 ppb, respectively, which was unique among the four seasons. In summer, the median and mean (± 1
281 SD) RH levels were 57.4 % and 57.6 (± 13.6) %, respectively, and the median and mean O₃ concentrations
282 were 46.9 ppb and 46.0 (± 18.3) ppb. It should be noted that the median and mean SO₂ concentrations
283 were 2.6 and 4.0 (± 3.7) ppb, respectively, which were the lowest in the year. Despite the low
284 concentrations of SO₂, there were considerable sulfate concentrations (Figs. 2 and 9), which can be
285 accounted for by fast SO₂-to-sulfate conversion. Although the rapid accumulation of secondary sulfate
286 during winter haze days in Beijing has been widely reported (Wang et al., 2014b; Zheng et al., 2015b),
287 the lowest SOR was observed during winter in the present study (Fig. 9a), which is consistent with
288 previous observations (Wang et al., 2005). On winter haze days, RH values of up to 73.6 % and PM_{2.5}
289 mass loadings of up to 375.3 $\mu\text{g m}^{-3}$ were observed. Therefore, AWC was not the limiting factor in SO₂-

290 to-sulfate conversion (Figs. 9b and 9e). The SO₂-to-sulfate conversion rate in winter could have been
291 limited by the reduced concentration of oxidants (Fig. 9c) as a result of both high emissions of the primary
292 pollutant NO (Fig. S9) and low solar radiation levels (Fig. 9f). Sulfate concentrations in winter were
293 comparable to those in summer, which might have been driven by high SO₂ concentrations in winter (Fig.
294 9d), despite slow SO₂-to-sulfate conversion. The lower boundary layer height in winter relative to other
295 seasons would also have encouraged the accumulation of both PM_{2.5} and its components, including sulfate
296 (Gao et al., 2015; Zhang et al., 2015). The SORs in spring and autumn were comparable and moderate,
297 possibly representing a transition in conditions between summer and winter.

298 For each season, four pollution scenarios were classified according to PM_{2.5} level. The lowest
299 25 %, 25–50 %, 50–75 %, and highest 25 % of pollution levels were defined as “clean”, “moderate
300 pollution”, “heavy pollution”, and “severe pollution”, respectively. The relative contributions of the seven
301 major known components of PM_{2.5} among the four pollution scenarios are shown in Fig. 10. In all four
302 seasons, the relative contribution of SNA increased with PM_{2.5} loading. This phenomenon has been
303 reported in previous studies, but data availability was limited in autumn (Xu et al., 2017) and winter
304 (Zheng et al., 2015b). The SOR increased consistently in all four seasons as pollution accumulated, where
305 both the highest value and strongest variability were observed in summer (Fig. 11a). Although SO₂ should
306 have reduced the SOR (Eq. 1), concurrent increases in primary SO₂ and SORs were observed (Figs. 11a
307 and 11b), indicating a significant increase in the SO₂-to-sulfate conversion rate with PM_{2.5} loading, which
308 offset the “dilution” effect (Eq. 1). Such variations in sulfate formation with pollution levels can be
309 accounted for by the corresponding variations in both O₃ concentrations and RH (Figs. 11c and 11d). In
310 all four seasons, RH increased consistently as pollution accumulated (Fig. 11d). O₃ concentrations
311 decreased consistently as pollution evolved in all of the seasons except for summer (Fig. 11c). The distinct
312 variations in O₃ during summer, imply strong photochemistry and high concentrations of OH, which
313 might result in a non-negligible contribution of gas phase reactions to the formation of sulfate. However,
314 gas phase reactions alone could not account for the rate of sulfate formation either in Beijing or globally
315 (Finlayson-Pitts and Pitts, 2000; He et al., 2018), due to the relatively slow reaction of SO₂ with OH. For
316 example, the lifetime of SO₂ with respect to OH oxidation is about 3–4 days, assuming a 24-h average
317 OH concentration of 1×10^6 molecules cm⁻³ and a pseudo-secondary-order rate constant of 10^{-12} cm³
318 molecule⁻¹ s⁻¹ (Brothers et al., 2010). However, the overall oxidation lifetime of SO₂ is on the order of
319 hours (Berglen et al., 2004; He et al., 2018). Overall, the increase in SO₂-to-sulfate conversion with PM_{2.5}

loading can be attributed to the self-catalytic nature of the multiphase formation of sulfate, i.e., both RH and PM_{2.5} increased continuously with the accumulation of PM_{2.5}, resulting in a rapid rise in AWC and providing greater reaction volume for further sulfate formation. Therefore, the increases in RH and PM_{2.5} could have compensated for the low concentration of oxidants, resulting in fast sulfate formation as pollution evolved. Particularly in summer, not only did both RH and O₃ concentrations increase as pollution evolved, but both RH and O₃ concentrations were generally above their respective thresholds at all pollution levels (dashed lines in Figs. 11c and 11d). This explains our observations of both the highest values and strongest dependence on pollution level for SORs in summer.

4 Conclusions

In this study, the annual mean concentration of PM_{2.5} in Beijing during 2012–2013 was 84.1 (± 63.1) $\mu\text{g m}^{-3}$, with clear seasonal and pollution level variations in its chemical components, highlighting the contribution of SNA formation to the accumulation of PM_{2.5} in all seasons. RH and O₃ concentrations were identified as two prerequisites for fast SO₂-to-sulfate conversion. RH above a threshold of ~45% greatly accelerated the conversion rate. A similar effect was also found for O₃ at a concentration threshold of ~35 ppb. Such dependences have interesting implications. First, they indicate a major role of the H₂O₂ route in sulfate formation, which might further indicate a major role of *in situ* sulfate production in the boundary layer, rather than in-cloud processes and intrusion from the free troposphere. Second, the observed dependences were also able to account for the seasonal and pollution level variations in SO₂-to-sulfate conversion rates. Both the highest value and strongest variability of SOR were observed in summer, which might be attributed to the highest values of O₃ concentrations and RH in summer. SO₂-to-sulfate conversion accelerated as pollution accumulated, which was primarily attributed to a shift from gas phase oxidation to the multiphase oxidation route, which is self-catalytic in nature. The increase in RH was able to offset the low concentration of oxidants under heavily polluted conditions, and resulted in increasingly fast SO₂-to-sulfate conversion as pollution accumulated. While our simultaneous observations of the SOR and concentrations of Fe and NO₂ could not exclude TMIs + O₂ and NO₂-based reactions, a reassessment of the relationships between sulfate formation, aerosol surface area, and the concentrations of Fe and NO₂ is necessary. Future quantitative studies of the relative contributions of different sulfate formation routes should include additional measurements, namely NH₃ for the proxy calculation of pH values, and H₂O₂ to confirm its contribution under different condition.

349 **Author contributions**

350 TZ designed the study. YHF, CXY, and TZ prepared the manuscript with input from all co-authors. YHF
351 and JXW collected and weighed the PM_{2.5} filter samples and carried out the analysis of the components
352 of PM_{2.5}. FFX carried out the measurement of water soluble Fe. YSW and MH provided the data for
353 gaseous pollutants, temperature, and RH. WLL provided the solar radiation data.

354 **Competing interests.**

355 The authors declare that they have no conflict of interest.

356 **Acknowledgements**

357 This work was supported by the National Natural Science Foundation Committee of China (91544000,
358 41121004, and 91744206). We also thank Dr. Robert Woodward-Massey for his kind help in English
359 writing.

360 **References**

361 Alexander, B., Park, R. J., Jacob, D. J., Li, Q. B., Yantosca, R. M., Savarino, J., Lee, C. C. W., and
362 Thiemens, M. H.: Sulfate formation in sea-salt aerosols: Constraints from oxygen isotopes, *J. Geophys.*
363 *Res.*, 110, <https://doi.org/10.1029/2004JD005659>, 2005.

364 Barth, M. C., Rasch, P. J., Kiehl, J. T., Benkovitz, C. M., and Schwartz, S. E.: Sulfur chemistry in the
365 National Center for Atmospheric Research Community Climate Model: Description, evaluation,
366 features, and sensitivity to aqueous chemistry, *J. Geophys. Res. Atmos.*, 105, 1387-1415,
367 <https://doi.org/10.1029/1999jd900773>, 2000.

368 Berglen, T. F., Berntsen, T. K., Isaksen, I. S. A., and Sundet, J. K.: A global model of the coupled
369 sulfur/oxidant chemistry in the troposphere: The sulfur cycle, *J. Geophys. Res. Atmos.*, 109,
370 <https://doi.org/10.1029/2003jd003948>, 2004.

371 Brothers, L. A., Dominguez, G., Abramian, A., Corbin, A., Bluen, B., and Thiemens, M. H.: Optimized
372 low-level liquid scintillation spectroscopy of S-35 for atmospheric and biogeochemical chemistry
373 applications, *Proc. Natl. Acad. Sci. U.S.A.*, 107, 5311-5316, <https://doi.org/10.1073/pnas.0901168107>,
374 2010.

375 Cheng, Y. F., Zheng, G. J., Wei, C., Mu, Q., Zheng, B., Wang, Z. B., Gao, M., Zhang, Q., He, K. B.,
376 Carmichael, G., Poschl, U., and Su, H.: Reactive nitrogen chemistry in aerosol water as a source of
377 sulfate during haze events in China, *Sci. adv.*, 2, <https://doi.org/10.1126/sciadv.1601530>, 2016.

378 Deguillaume, L., Leriche, M., Desboeufs, K., Mailhot, G., George, C., and Chaumerliac, N.: Transition
379 metals in atmospheric liquid phases: Sources, reactivity, and sensitive parameters, *Chem. Rev.*, 105,
380 3388-3431, <https://doi.org/10.1002/chin.200549218>, 2005.

381 Ding, J., Zhao, P., Su, J., Dong, Q., Du, X., and Zhang, Y.: Aerosol pH and its driving factors in Beijing,
382 *Atmos. Chem. Phys.*, 19, 7939-7954, <https://doi.org/10.5194/acp-19-7939-2019>, 2019.

383 Ervens, B.: Modeling the processing of aerosol and trace gases in clouds and fogs, *Chem. Rev.*, 115,
384 <https://doi.org/10.1021/cr5005887>, 2015.

385 Finlayson-Pitts, B. J., and Pitts, J. N. Jr.: Chemistry of the upper and lower atmosphere: Theory,
386 experiments, and applications, Academic Press, San Diego, California, 2000.

387 Fu, A. Y.: Study on peroxide concentration and its influence factors in the urban atmosphere, Master,
388 College of Environmental and Resource Sciences, Zhejiang University, Hangzhou, China, 2014 (in
389 Chinese).

390 Gao, Y., Zhang, M., Liu, Z., Wang, L., Wang, P., Xia, X., Tao, M., and Zhu, L.: Modeling the feedback
391 between aerosol and meteorological variables in the atmospheric boundary layer during a severe fog-
392 haze event over the North China Plain, *Atmos. Chem. Phys.*, 15, 4279-4295,
393 <https://doi.org/10.5194/acp-15-4279-2015>, 2015.

394 Gleason, J. F., Sinha, A., and Howard, C. J.: Kinetics of the gas phase reaction $\text{HOSO}_2 + \text{O}_2 \rightarrow \text{HO}_2 + \text{SO}_3$,
395 *J. Phys. Chem.*, 91, 719-724, <https://doi.org/10.1021/j100287a045>, 1987.

396 Guo, H., Weber, R. J., and Nenes, A.: High levels of ammonia do not raise fine particle pH sufficiently
397 to yield nitrogen oxide-dominated sulfate production, *Sci. Rep.*, 7, 12109,
398 <https://doi.org/10.1038/s41598-017-11704-0>, 2017.

399 Han, L., Cheng, S., Zhuang, G., Ning, H., Wang, H., Wei, W., and Zhao, X.: The changes and long-range
400 transport of $\text{PM}_{2.5}$ in Beijing in the past decade, *Atmos. Environ.*, 110, 186-195,
401 <https://doi.org/10.1016/j.atmosenv.2015.03.013>, 2015.

402 Harris, E., Sinha, B., van Pinxteren, D., Tilgner, A., Fomba, K. W., Schneider, J., Roth, A., Gnauk, T.,
403 Fahlbusch, B., Mertes, S., Lee, T., Collett, J., Foley, S., Borrmann, S., Hoppe, P., and Herrmann, H.:

404 Enhanced role of transition metal ion catalysis during in-cloud oxidation of SO₂, *Science*, 340, 727-
405 730, <https://doi.org/10.1126/science.1230911>, 2013.

406 Harris, E., Sinha, B., van Pinxteren, D., Schneider, J., Poulain, L., Collett, J., D'Anna, B., Fahlbusch, B.,
407 Foley, S., Fomba, K. W., George, C., Gnauk, T., Henning, S., Lee, T., Mertes, S., Roth, A., Stratmann,
408 F., Borrmann, S., Hoppe, P., and Herrmann, H.: In-cloud sulfate addition to single particles resolved
409 with sulfur isotope analysis during HCCT-2010, *Atmos. Chem. Phys.*, 14, 4219-4235,
410 <https://doi.org/10.5194/acp-14-4219-2014>, 2014.

411 He, H., Wang, Y., Ma, Q., Ma, J., Chu, B., Ji, D., Tang, G., Liu, C., Zhang, H., and Hao, J.: Mineral dust
412 and NO_x promote the conversion of SO₂ to sulfate in heavy pollution days, *Sci. Rep.*, 4,
413 <https://doi.org/10.1038/srep04172>, 2014.

414 He, P., Alexander, B., Geng, L., Chi, X., Fan, S., Zhan, H., Kang, H., Zheng, G., Cheng, Y., Su, H., Liu,
415 C., and Xie, Z.: Isotopic constraints on heterogeneous sulfate production in Beijing haze, *Atmos. Chem.*
416 *Phys.*, 18, 5515-5528, <https://doi.org/10.5194/acp-18-5515-2018>, 2018.

417 Hu, M., Guo, S., Peng, J.-f., and Wu, Z.-j.: Insight into characteristics and sources of PM_{2.5} in the Beijing-
418 Tianjin-Hebei region, China, *Nati. Sci. Rew.*, 2, 257-258, <https://doi.org/10.1093/nsr/nwv003>, 2015.

419 Huang, R. J., Zhang, Y. L., Bozzetti, C., Ho, K. F., Cao, J. J., Han, Y. M., Daellenbach, K. R., Slowik, J.
420 G., Platt, S. M., Canonaco, F., Zotter, P., Wolf, R., Pieber, S. M., Bruns, E. A., Crippa, M., Ciarelli, G.,
421 Piazzalunga, A., Schwikowski, M., Abbaszade, G., Schnelle-Kreis, J., Zimmermann, R., An, Z. S.,
422 Szidat, S., Baltensperger, U., El Haddad, I., and Prevot, A. S. H.: High secondary aerosol contribution
423 to particulate pollution during haze events in China, *Nature*, 514, 218-222,
424 <https://doi.org/10.1038/nature13774>, 2014a.

425 Lelieveld, J., Gromov, S., Pozzer, A., and Taraborrelli, D.: Global tropospheric hydroxyl distribution,
426 budget and reactivity, *Atmos. Chem. Phys.*, 16, 12477-12493, [https://doi.org/10.5194/acp-16-12477-](https://doi.org/10.5194/acp-16-12477-2016)
427 [2016](https://doi.org/10.5194/acp-16-12477-2016), 2016.

428 Li, L., Hoffmann, M. R., and Colussi, A. J.: The role of nitrogen dioxide in the production of sulfate
429 during Chinese haze-aerosol episodes, *Environ. Sci. Technol.*, 52,
430 <https://doi.org/10.1021/acs.est.7b05222>, 2018.

431 Li, Y. R., Ye, C. X., Liu, J., Zhu, Y., Wang, J. X., Tan, Z. Q., Lin, W. L., Zeng, L. M., and Zhu, T.:
432 Observation of regional air pollutant transport between the megacity Beijing and the North China Plain,
433 *Atmos. Chem. Phys.*, 16, 14265-14283, <https://doi.org/10.5194/acp-16-14265-2016>, 2016.

434 Liang, P., Zhu, T., Fang, Y., Li, Y., Han, Y., Wu, Y., Hu, M., and Wang, J.: The role of meteorological
435 conditions and pollution control strategies in reducing air pollution in Beijing during APEC 2014 and
436 Victory Parade 2015, *Atmos. Chem. Phys.*, 17, 13921-13940, [https://doi.org/10.5194/acp-17-13921-](https://doi.org/10.5194/acp-17-13921-2017)
437 [2017](https://doi.org/10.5194/acp-17-13921-2017), 2017.

438 Liu, M., Song, Y., Zhou, T., Xu, Z., Yan, C., Zheng, M., Wu, Z., Hu, M., Wu, Y., and Zhu, T.: Fine
439 particle pH during severe haze episodes in northern China, *Geophys. Res. Lett.*, 44, 5213-5221,
440 <https://doi.org/10.1002/2017GL073210>, 2017a.

441 Liu, X., Sun, K., Qu, Y., Hu, M., Sun, Y., Zhang, F., and Zhang, Y.: Secondary formation of sulfate and
442 nitrate during a haze episode in megacity Beijing, China, *Aerosol Air Qual. Res.*, 2246 - 2257,
443 <https://doi.org/10.4209/aaqr.2014.12.0321>, 2015.

444 Liu, Y. C., Wu, Z. J., Wang, Y., Xiao, Y., Gu, F. T., Zheng, J., Tan, T. Y., Shang, D. J., Wu, Y. S., Zeng,
445 L. M., Hu, M., Bateman, A. P., and Martin, S. T.: Submicrometer particles are in the liquid state during
446 heavy haze episodes in the urban atmosphere of Beijing, China, *Environ. Sci. Technol. Lett.*, 4, 427-
447 432, <https://doi.org/10.1021/acs.estlett.7b00352>, 2017b.

448 Lu, X., Chen, N., Wang, Y., Cao, W., Zhu, B., Yao, T., Fung, J. C. H., and Lau, A. K. H.: Radical budget
449 and ozone chemistry during autumn in the atmosphere of an urban aite in central China: RO_x budgets
450 and O₃ in central China, *J. Geophys. Res. Atmos.*, 122, 3672-3685,
451 <https://doi.org/10.1002/2016JD025676>, 2017.

452 Lv, B., Zhang, B., and Bai, Y.: A systematic analysis of PM_{2.5} in Beijing and its sources from
453 2000 to 2012, *Atmos. Environ.*, 124, 98-108, <https://doi.org/10.1016/j.atmosenv.2015.09.031>, 2016.

454 Ma, J., Chu, B., Liu, J., Liu, Y., Zhang, H., and He, H.: NO_x promotion of SO₂ conversion to sulfate: An
455 important mechanism for the occurrence of heavy haze during winter in Beijing, *Environ. Pollut.*, 233,
456 662, <https://doi.org/10.1016/j.envpol.2017.10.103>, 2018.

457 Pan, X. L., Yan, P., Tang, J., Ma, J. Z., Wang, Z. F., Gbaguidi, A., and Sun, Y. L.: Observational study
458 of influence of aerosol hygroscopic growth on scattering coefficient over rural area near Beijing mega-
459 city, *Atmos. Chem. Phys.*, 9, 7519-7530, <https://doi.org/10.5194/acp-9-7519-2009>, 2009.

460 Quan, J., Liu, Q., Li, X., Gao, Y., Jia, X., Sheng, J., and Liu, Y.: Effect of heterogeneous aqueous reactions
461 on the secondary formation of inorganic aerosols during haze events, *Atmos. Environ.*, 122, 306-312,
462 <https://doi.org/10.1016/j.atmosenv.2015.09.068>, 2015.

463 Quan, J. N., Tie, X. X., Zhang, Q., Liu, Q., Li, X., Gao, Y., and Zhao, D. L.: Characteristics of heavy
464 aerosol pollution during the 2012-2013 winter in Beijing, China, *Atmos. Environ.*, 88, 83-89,
465 <https://doi.org/10.1016/j.atmosenv.2014.01.058>, 2014.

466 Russell, L. M., and Ming, Y.: Deliquescence of small particles, *J. Chem. Phys.*, 116, 311,
467 <https://doi.org/10.1063/1.1420727>, 2002.

468 Sarwar, G., Simon, H., Fahey, K., Mathur, R., Goliff, W. S., and Stockwell, W. R.: Impact of sulfur
469 dioxide oxidation by Stabilized Criegee Intermediate on sulfate, *Atmos. Environ.*, 85, 204-214,
470 <https://doi.org/10.1016/j.atmosenv.2013.12.013>, 2014.

471 Seinfeld, J. H., and Pandis, S. N.: *Atmospheric chemistry and physics: From air pollution to climate*
472 *change*, Second ed., John Wiley & Sons, New Jersey, 2006.

473 Shen, X. H., Lee, T. Y., Guo, J., Wang, X. F., Li, P. H., Xu, P. J., Wang, Y., Ren, Y., Wang, W., Wang,
474 T., Li, Y., Cam, S. A., and Collett, J. L.: Aqueous phase sulfate production in clouds in eastern China,
475 *Atmos. Environ.*, 62, 502-511, <https://doi.org/10.1016/j.atmosenv.2012.07.079>, 2012.

476 Sievering, H., Caine, J., Harvey, M., McGregor, J., Nichol, S., and Quinn, P.: Aerosol non-sea-salt sulfate
477 in the remote marine boundary layer under clear-sky and normal cloudiness conditions: Ocean-derived
478 biogenic alkalinity enhances sea-salt sulfate production by ozone oxidation, *J. Geophys. Res. Atmos.*,
479 109, <https://doi.org/10.1029/2003jd004315>, 2004.

480 Sun, Y., Wang, Z., Fu, P., Jiang, Q., Yang, T., Li, J., and Ge, X.: The impact of relative humidity on
481 aerosol composition and evolution processes during wintertime in Beijing, China, *Atmos. Environ.*, 77,
482 927-934, <https://doi.org/10.1016/j.atmosenv.2013.06.019>, 2013.

483 Sun, Y. L., Zhuang, G. S., Tang, A. H., Wang, Y., and An, Z. S.: Chemical characteristics of PM_{2.5} and
484 PM₁₀ in haze-fog episodes in Beijing, *Environ. Sci. Technol.*, 40, 3148-3155,
485 <https://doi.org/10.1021/es051533g>, 2006.

486 Sun, Y. L., Jiang, Q., Wang, Z. F., Fu, P. Q., Li, J., Yang, T., and Yin, Y.: Investigation of the sources
487 and evolution processes of severe haze pollution in Beijing in January 2013, *J. Geophys. Res. Atmos.*,
488 119, 4380-4398, <https://doi.org/10.1002/2014JD021641>, 2014.

489 Vereecken, L., Harder, H., and Novelli, A.: The reaction of Criegee intermediates with NO, RO₂, and
490 SO₂, and their fate in the atmosphere, *Phys. Chem. Chem. Phys.*, 14, 14682,
491 <https://doi.org/10.1039/c2cp42300f>, 2012.

492 Wang, G. H., Zhang, R. Y., Gomez, M. E., Yang, L. X., Zamora, M. L., Hu, M., Lin, Y., Peng, J. F., Guo,
493 S., Meng, J. J., Li, J. J., Cheng, C. L., Hu, T. F., Ren, Y. Q., Wang, Y. S., Gao, J., Cao, J. J., An, Z. S.,
494 Zhou, W. J., Li, G. H., Wang, J. Y., Tian, P. F., Marrero-Ortiz, W., Secret, J., Du, Z. F., Zheng, J.,
495 Shang, D. J., Zeng, L. M., Shao, M., Wang, W. G., Huang, Y., Wang, Y., Zhu, Y. J., Li, Y. X., Hu, J.
496 X., Pan, B., Cai, L., Cheng, Y. T., Ji, Y. M., Zhang, F., Rosenfeld, D., Liss, P. S., Duce, R. A., Kolb,
497 C. E., and Molina, M. J.: Persistent sulfate formation from London Fog to Chinese haze, *Proc. Natl.*
498 *Acad. Sci. U.S.A.*, 113, 13630-13635, <https://doi.org/10.1073/pnas.1616540113>, 2016.

499 Wang, Y., Zhuang, G., Tang, A., Yuan, H., Sun, Y., Chen, S., and Zheng, A.: The ion chemistry and the
500 source of PM_{2.5} aerosol in Beijing, *Atmos. Environ.*, 39, 3771-3784,
501 <https://doi.org/10.1016/j.atmosenv.2005.03.013>, 2005.

502 Wang, Y., Zhang, Q., Jiang, J., Zhou, W., Wang, B., He, K., Duan, F., Zhang, Q., Philip, S., and Xie, Y.:
503 Enhanced sulfate formation during China's severe winter haze episode in January 2013 missing from
504 current models, *J. Geophys. Res. Atmos.*, 119, 410,425-410,440, <https://doi.org/10.1002/2013JD021426>,
505 2014a.

506 Wang, Y. S., Yao, L., Wang, L. L., Liu, Z. R., Ji, D. S., Tang, G. Q., Zhang, J. K., Sun, Y., Hu, B., and
507 Xin, J. Y.: Mechanism for the formation of the January 2013 heavy haze pollution episode over central
508 and eastern China, *Sci. China Earth Sci.*, 57, 14-25, <https://doi.org/10.1007/s11430-013-4773-4>, 2014b.

509 Warneck, P.: The oxidation of sulfur(IV) by reaction with iron(III): a critical review and data analysis,
510 *Phys. Chem. Chem. Phys.*, 20, 4020-4037, <https://doi.org/10.1039/c7cp07584g>, 2018.

511 Xie, Y., Ding, A., Nie, W., Mao, H., Qi, X., Huang, X., Xu, Z., Kerminen, V. M., Pet ä ä T., and Chi, X.:
512 Enhanced sulfate formation by nitrogen dioxide: Implications from in-situ observations at the SORPES
513 Station, *J. Geophys. Res. Atmos.*, 120, 12679-12694, <https://doi.org/10.1002/2015JD023607>, 2015.

514 Xu, F., Qiu, X., Hu, X., Shang, Y., Pardo, M., Fang, Y., Wang, J., Rudich, Y., and Zhu, T.: Effects on IL-
515 1 β signaling activation induced by water and organic extracts of fine particulate matter (PM_{2.5}) in vitro,
516 *Environ. Pollut.*, 237, 592-600, <https://doi.org/10.1016/j.envpol.2018.02.086>, 2018.

517 Xu, L., Duan, F., He, K., Ma, Y., Zhu, L., Zheng, Y., Huang, T., Kimoto, T., Ma, T., Li, H., Ye, S., Yang,
518 S., Sun, Z., and Xu, B.: Characteristics of the secondary water-soluble ions in a typical autumn haze in
519 Beijing, *Environ. Pollut.*, 227, 296-305, <https://doi.org/10.1016/j.envpol.2017.04.076>, 2017.

520 Yang, Y. R., Liu, X. G., Qu, Y., An, J. L., Jiang, R., Zhang, Y. H., Sun, Y. L., Wu, Z. J., Zhang, F., Xu,
521 W. Q., and Ma, Q. X.: Characteristics and formation mechanism of continuous hazes in China: a case

522 study during the autumn of 2014 in the North China Plain, *Atmos. Chem. Phys.*, 15, 8165-8178,
523 <https://doi.org/10.5194/acp-15-8165-2015>, 2015.

524 Ye, C., Liu, P., Ma, Z., Xue, C., Zhang, C., Zhang, Y., Liu, J., Liu, C., Sun, X., and Mu, Y.: High H₂O₂
525 concentrations observed during haze periods in wintertime of Beijing: Importance of H₂O₂-oxidation
526 in sulfate formation, *Environ. Sci. Technol. Lett.*, <https://doi.org/10.1021/acs.estlett.8b00579>, 2018.

527 Yu, T., Zhao, D., Song, X., and Zhu, T.: NO₂-initiated multiphase oxidation of SO₂ by O₂ on CaCO₃
528 particles, *Atmos. Chem. Phys.*, 18, 6679-6689, <https://doi.org/10.5194/acp-18-6679-2018>, 2018.

529 Zhang, Q., Quan, J. N., Tie, X. X., Li, X., Liu, Q., Gao, Y., and Zhao, D. L.: Effects of meteorology and
530 secondary particle formation on visibility during heavy haze events in Beijing, China, *Sci. Total.*
531 *Environ.*, 502, 578-584, <https://doi.org/10.1016/j.scitotenv.2014.09.079>, 2015.

532 Zhang, R., Jing, J., Tao, J., Hsu, S. C., Wang, G., Cao, J., Lee, C. S. L., Zhu, L., Chen, Z., Zhao, Y., and
533 Shen, Z.: Chemical characterization and source apportionment of PM_{2.5} in Beijing: Seasonal
534 perspective, *Atmos. Chem. Phys.*, 13, 7053-7074, <https://doi.org/10.5194/acp-13-7053-2013>, 2013.

535 Zhang, R., Sun, X. S., Shi, A. J., Huang, Y. H., Yan, J., Nie, T., Yan, X., and Li, X.: Secondary inorganic
536 aerosols formation during haze episodes at an urban site in Beijing, China, *Atmos. Environ.*, 177, 275-
537 282, <https://doi.org/10.1016/j.atmosenv.2017.12.031>, 2018.

538 Zhang, X. Y., Gong, S. L., Shen, Z. X., Mei, F. M., Xi, X. X., Liu, L. C., Zhou, Z. J., Wang, D., Wang,
539 Y. Q., and Cheng, Y.: Characterization of soil dust aerosol in China and its transport and distribution
540 during 2001 ACE-Asia: 1. Network observations, *J. Geophys. Res.*, 108,
541 <https://doi.org/10.1029/2002jd002632>, 2003.

542 Zhao, D., Song, X., Zhu, T., Zhang, Z., Liu, Y., and Shang, J.: Multiphase oxidation of SO₂ by NO₂ on
543 CaCO₃ particles, *Atmos. Chem. Phys.*, 18, 2481-2493, <https://doi.org/10.5194/acp-18-2481-2018>,
544 2018.

545 Zheng, B., Zhang, Q., Zhang, Y., He, K. B., Wang, K., Zheng, G. J., Duan, F. K., Ma, Y. L., and Kimoto,
546 T.: Heterogeneous chemistry: a mechanism missing in current models to explain secondary inorganic
547 aerosol formation during the January 2013 haze episode in North China, *Atmos. Chem. Phys.*, 15,
548 2031-2049, <https://doi.org/10.5194/acp-15-2031-2015>, 2015a.

549 Zheng, G. J., Duan, F. K., Su, H., Ma, Y. L., Cheng, Y., Zheng, B., Zhang, Q., Huang, T., Kimoto, T.,
550 Chang, D., Poschl, U., Cheng, Y. F., and He, K. B.: Exploring the severe winter haze in Beijing: the

551 impact of synoptic weather, regional transport and heterogeneous reactions, *Atmos. Chem. Phys.*, 15,
552 2969-2983, <https://doi.org/10.5194/acp-15-2969-2015>, 2015b.

553 Zheng, M., Salmon, L. G., Schauer, J. J., Zeng, L. M., Kiang, C. S., Zhang, Y. H., and Cass, G. R.:
554 Seasonal trends in PM_{2.5} source contributions in Beijing, China, *Atmos. Environ.*, 39, 3967-3976,
555 <https://doi.org/10.1016/j.atmosenv.2005.03.036>, 2005.

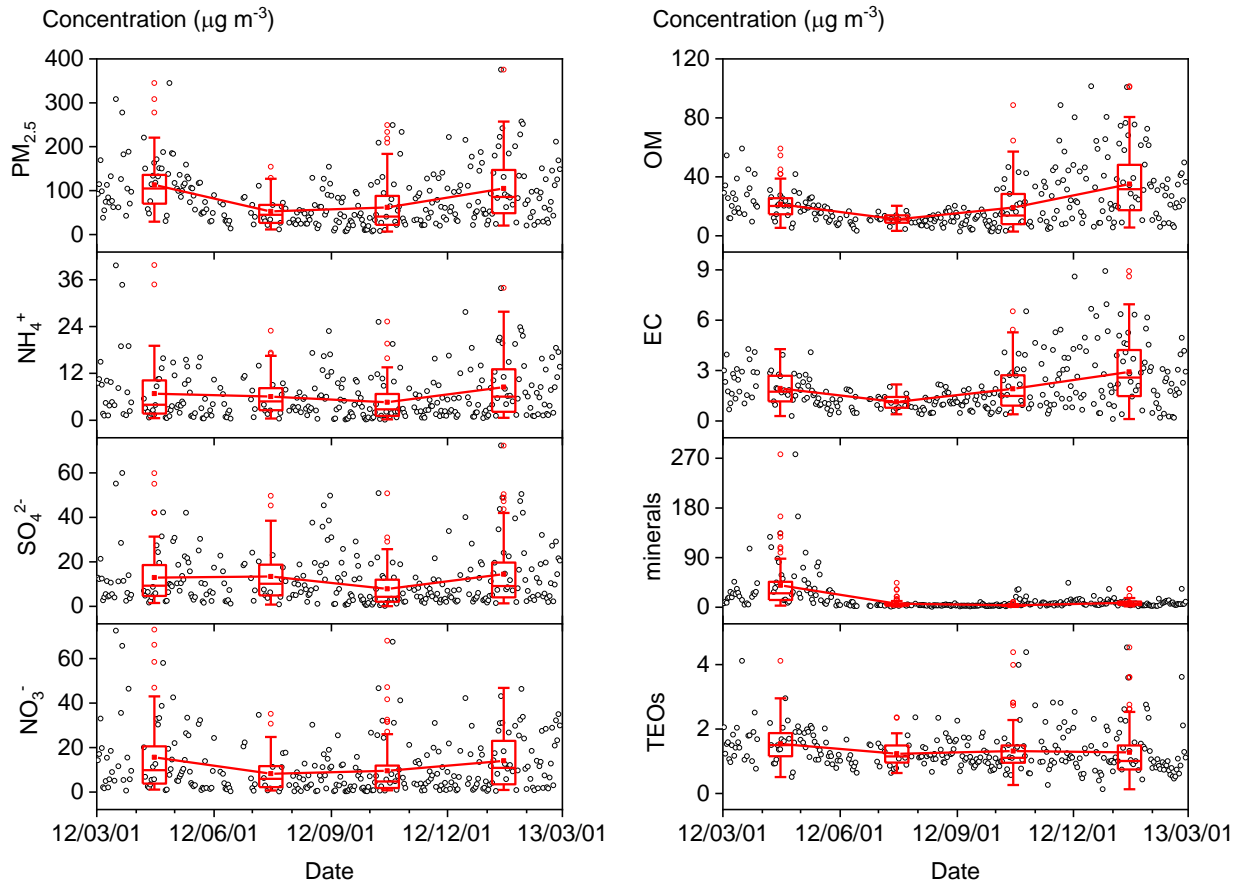
556 Zhu, T., Shang, J., and Zhao, D. F.: The roles of heterogeneous chemical processes in the formation of an
557 air pollution complex and gray haze, *Sci. China Chem.*, 54, 145-153, <https://doi.org/10.1007/s11426-010-4181-y>, 2011.

559 Zhuang, G. S., Guo, J. H., Yuan, H., and Zhao, C. Y.: The compositions, sources, and size distribution of
560 the dust storm from China in spring of 2000 and its impact on the global environment, *Chinese. Sci. Bull.*, 46, 895-901, <https://doi.org/10.1007/BF02900460>, 2001.

562



566 **Figure 1.** Sample sites in this study (red stars): (a) Peking University and (b) Beijing Meteorological Observatory.



567

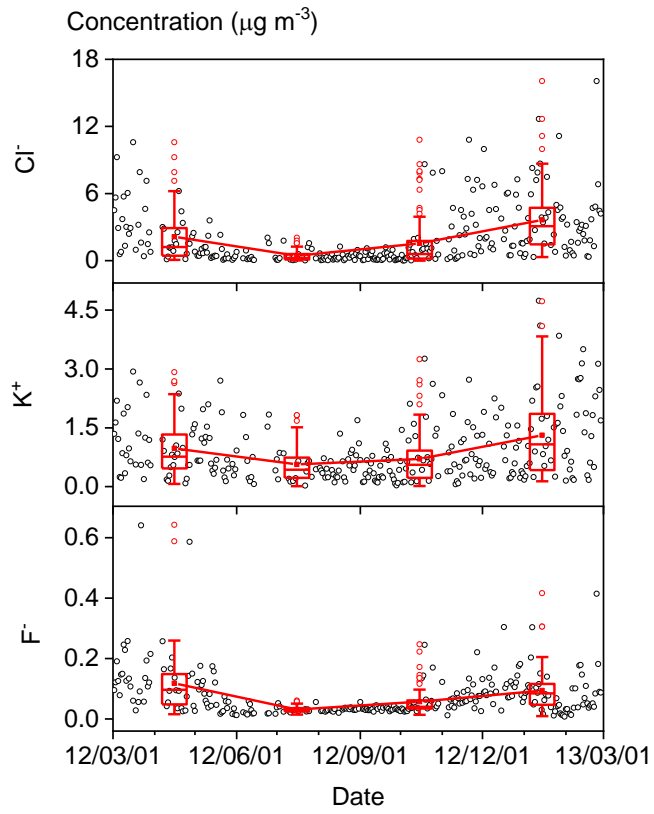
568

569

570

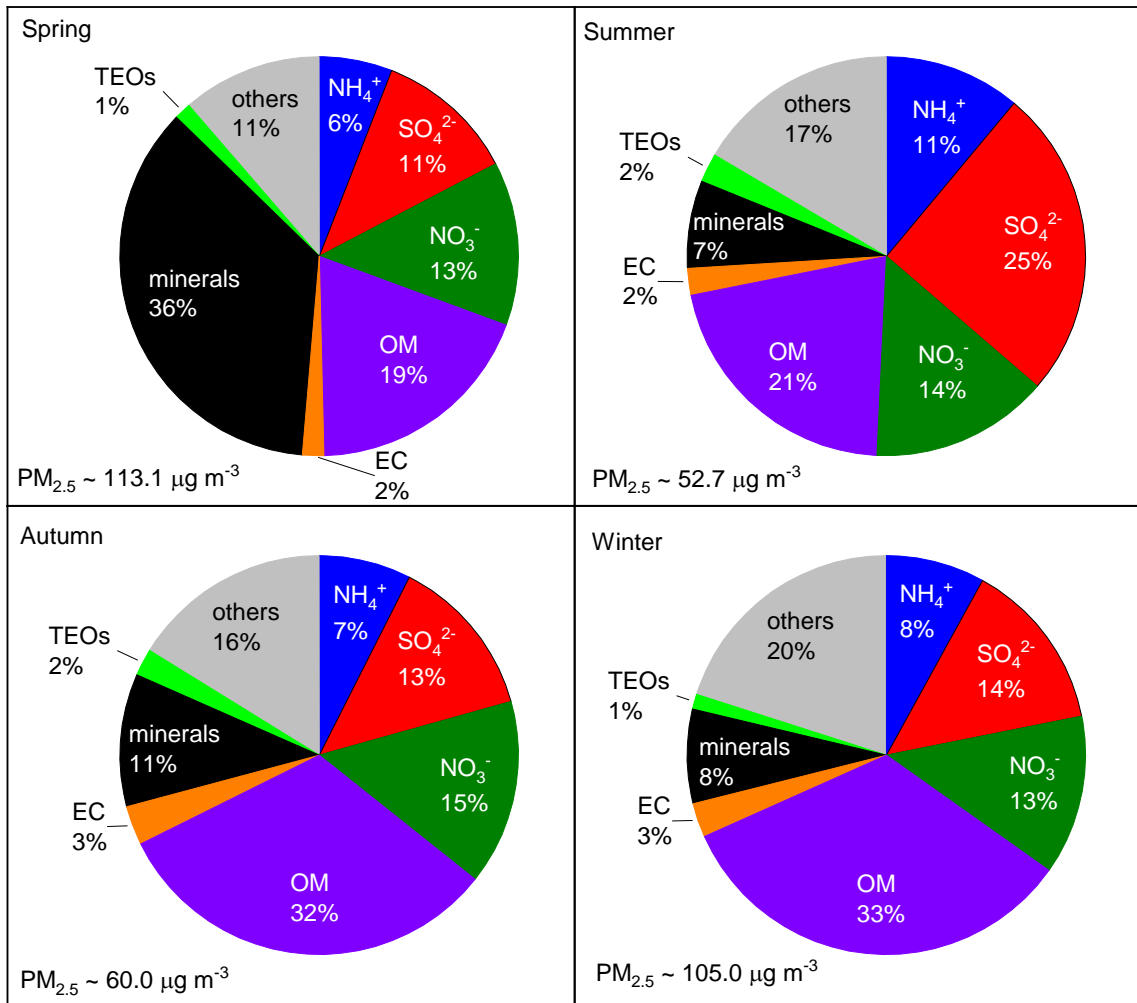
571

Figure 2. Time series of fine particulate matter (PM_{2.5}) concentrations and its seven major **known** components from March 2012 to February 28 2013 (open black circles). The boxes represent, from top to bottom, the 75th, 50th, and 25th percentiles for each season. The whiskers, solid red squares, and open red circles represent 1.5 times the interquartile range (IQR), seasonal mean values, and outlier data points, respectively.



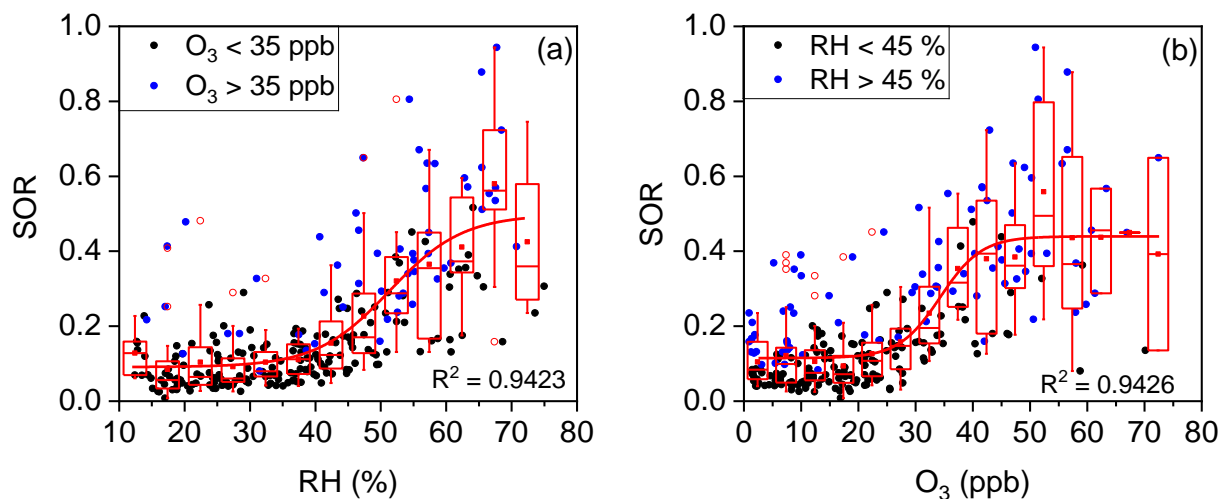
572

573 **Figure 3.** Time series of Cl⁻, K⁺, and F⁻ from 1 March 1 2012 to February 28 2013.



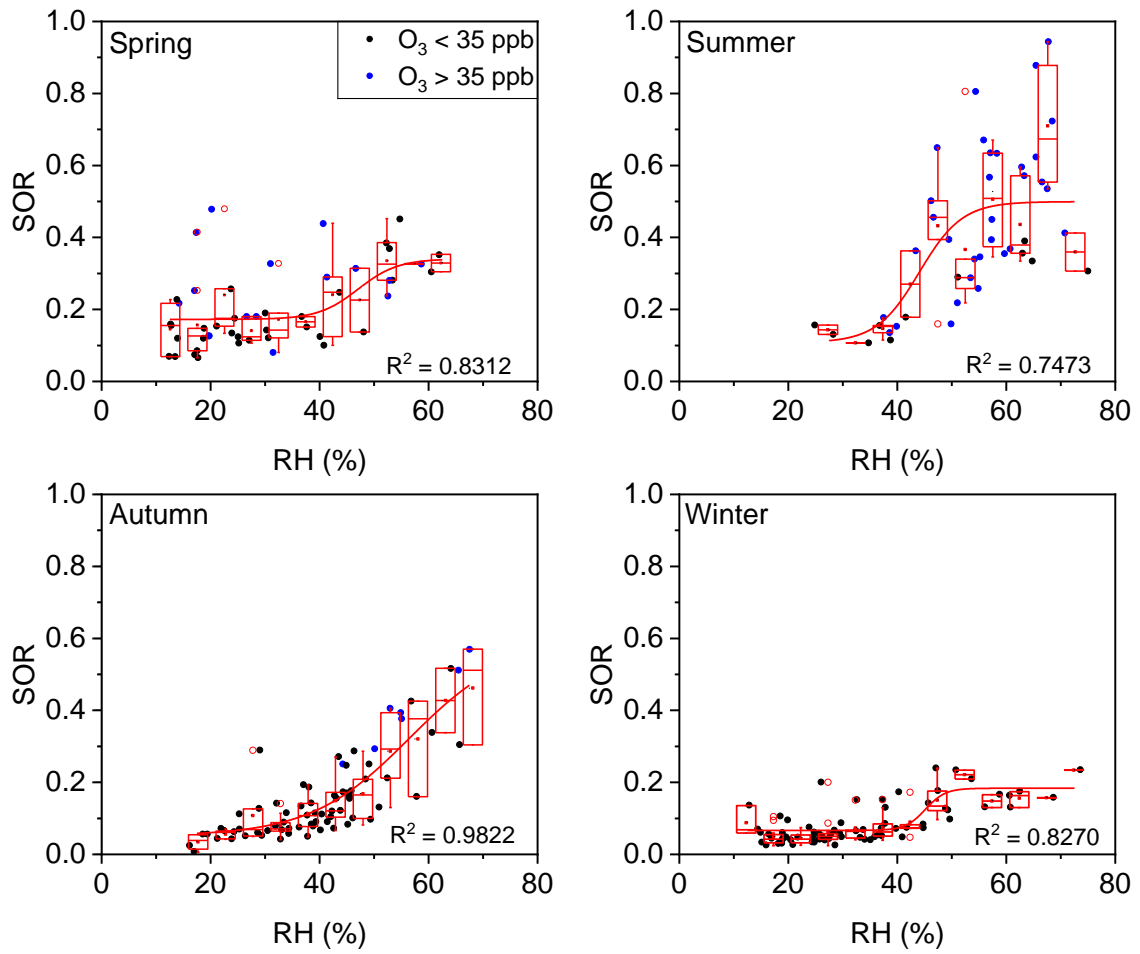
574

575 **Figure 4.** Seasonal variations in PM_{2.5} and its eight major components from March 1 2012 to February 28 2013



576

577 **Figure 5.** (a) Plot of the sulfur oxidation ratio (SOR) against relative humidity (RH) grouped by O_3 concentration. The solid
 578 blue circles represent $O_3 > 35$ ppb and the solid black circles represent $O_3 < 35$ ppb. (b) Plot of the SOR against O_3 grouped
 579 by RH. The solid blue circles represent $RH > 45$ % and the solid black circles represent $RH < 45$ %. The boxes represent, from
 580 top to bottom, the 75th, 50th, and 25th percentiles in each bin ($\Delta RH = 5$ %; $\Delta O_3 = 5$ ppb). The whiskers, solid red squares, and
 581 open red circles represent 1.5 times the IQR, mean values, and outlier data points, respectively. The red lines are best fits to
 582 mean values based on a sigmoid function. Data for days with rain or snow were excluded from these plots.



583

584

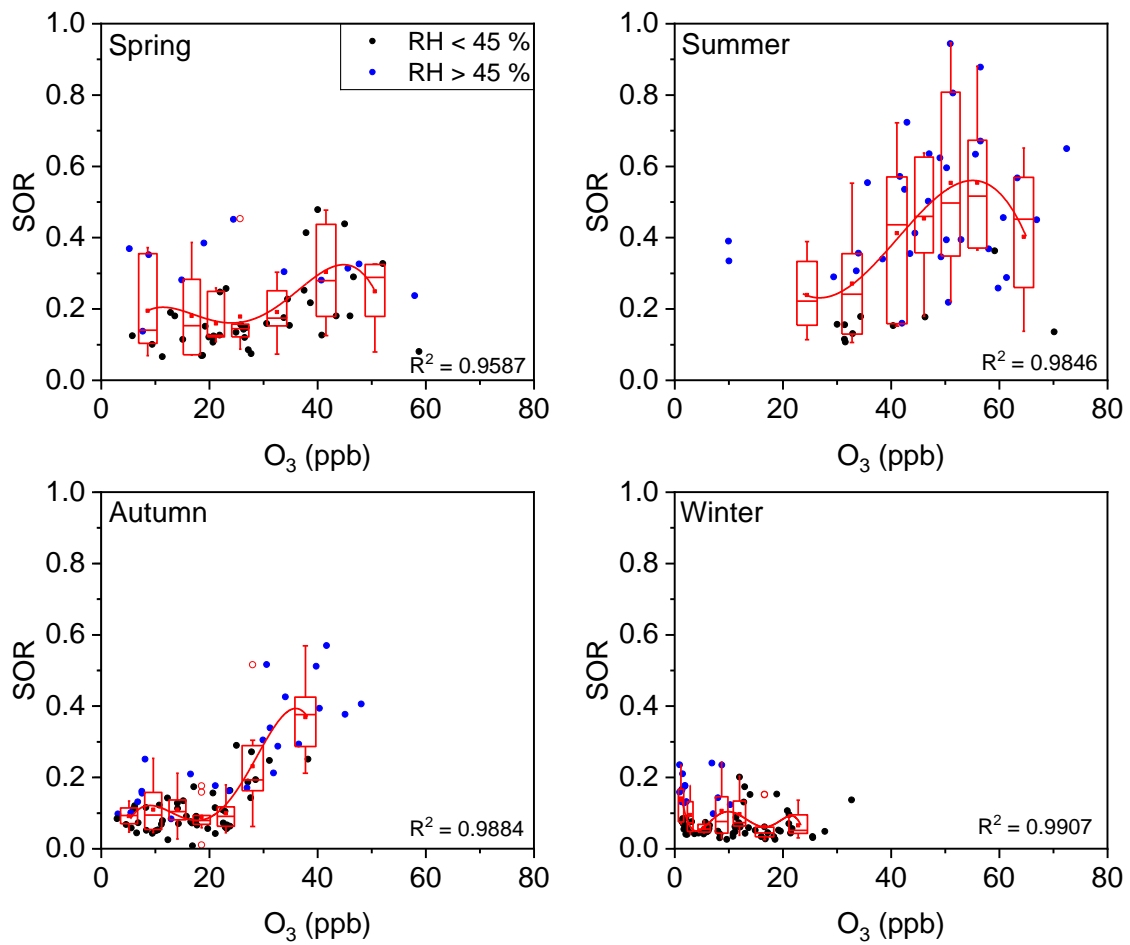
585

586

587

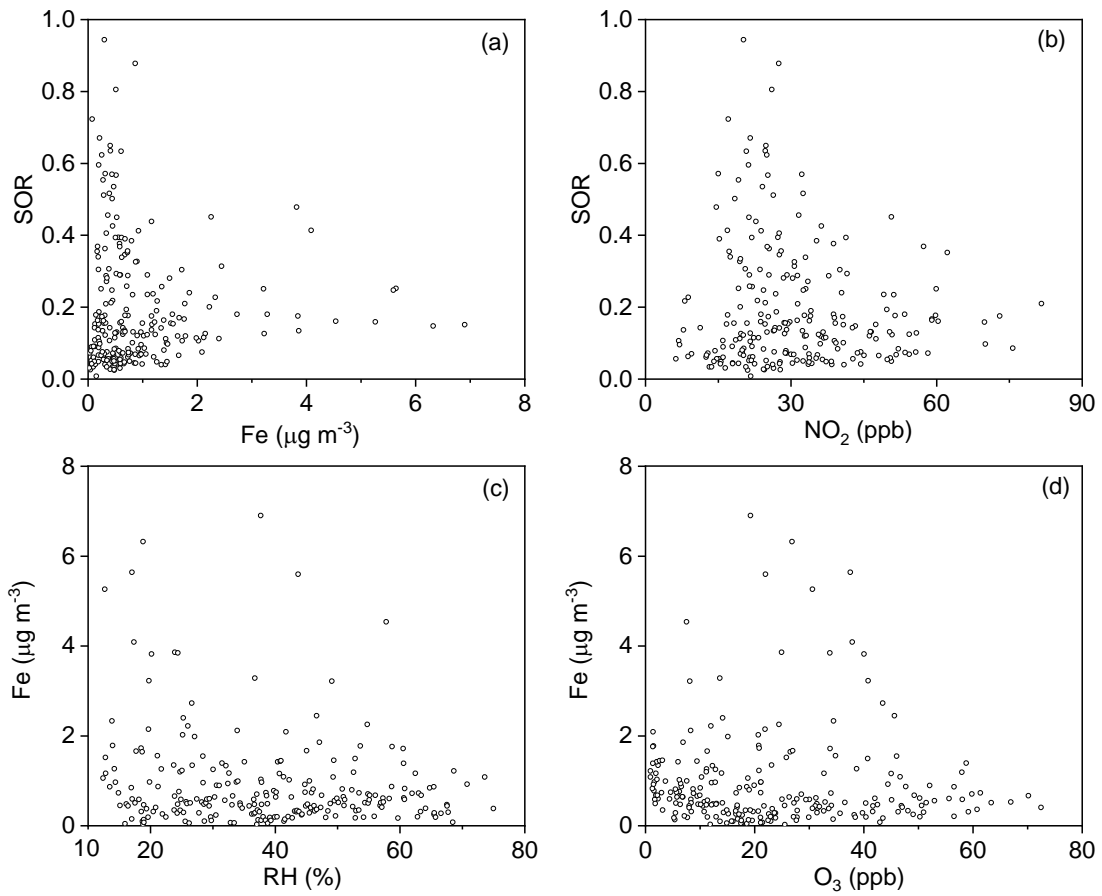
588

Figure 6. Plot of SOR against RH grouped by O₃ concentration in four seasons. The solid blue circles represent O₃ > 35 ppb and the solid black circles represent O₃ < 35 ppb. The boxes represent, from top to bottom, the 75th, 50th, and 25th percentiles in each bin (ΔRH = 5 %). The whiskers, solid red squares, and open red circles represent 1.5 times the IQR, mean values, and outlier data points, respectively. The red lines are best fits to mean values based on a sigmoid function. Data for days with rain or snow were excluded from these plots.



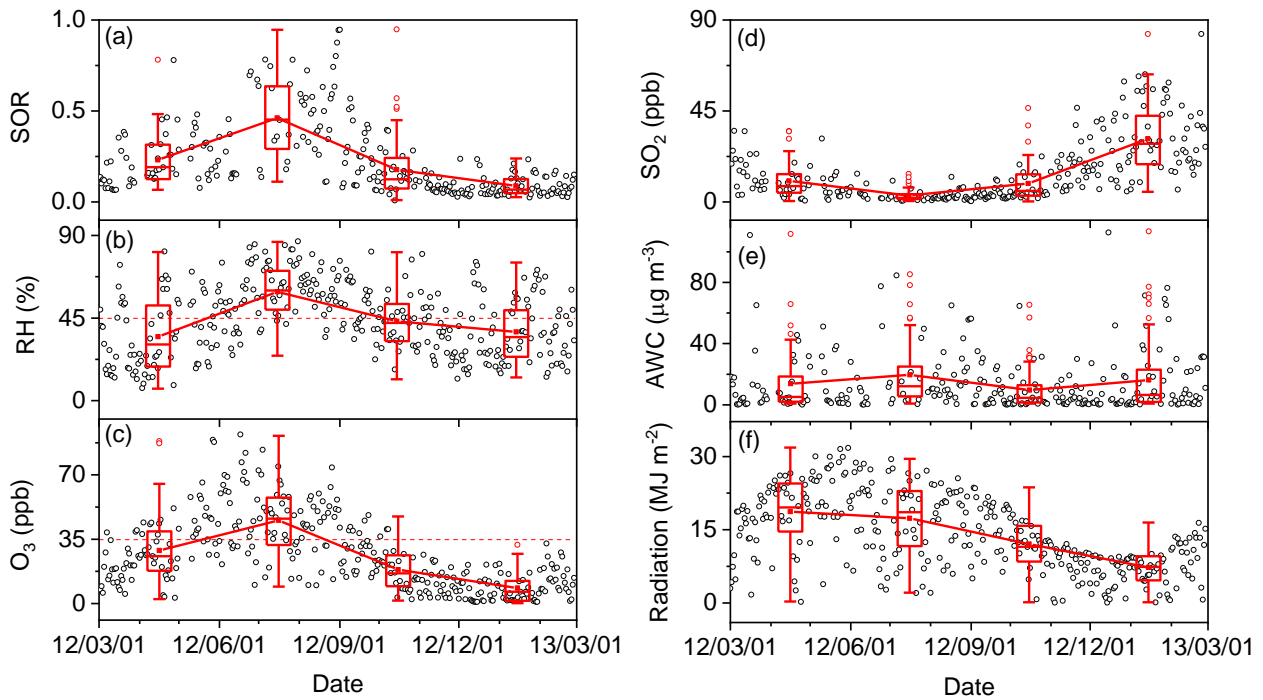
589

590 **Figure 7.** Plot of the SOR against O₃ grouped by RH. The solid blue circles represent RH > 45 % and the solid black circles
 591 represent RH < 45 %. The boxes represent, from top to bottom, the 75th, 50th, and 25th percentiles in each bin. The bin widths
 592 were set such that there were an approximately equal number of data points in each bin. The whiskers, solid red squares, and open red
 593 circles represent 1.5 times the IQR, mean values, and outlier data points, respectively. The red lines are best fits to mean values
 594 based on polynomial functions. Data for days with rain or snow were excluded from these plots.



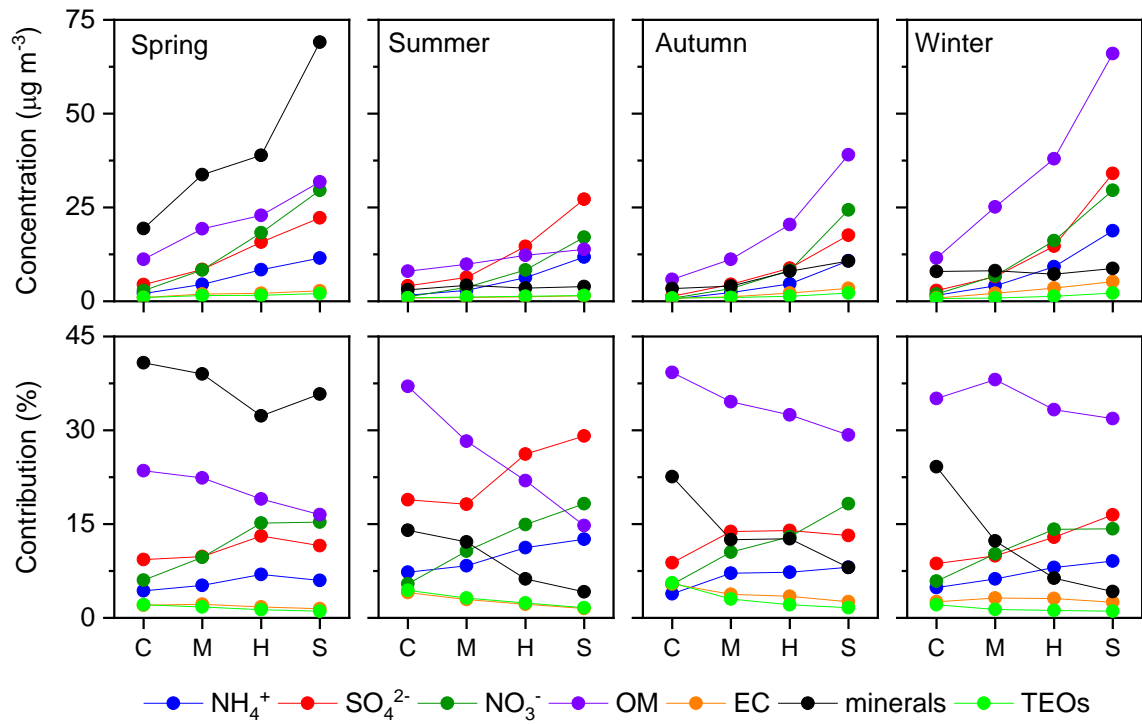
595

596 **Figure 8.** Plots of SORs against (a) Fe and (b) NO_2 . Plots of Fe against (c) RH and (d) O_3 . Data for days with rain or snow
 597 were excluded from these plots.



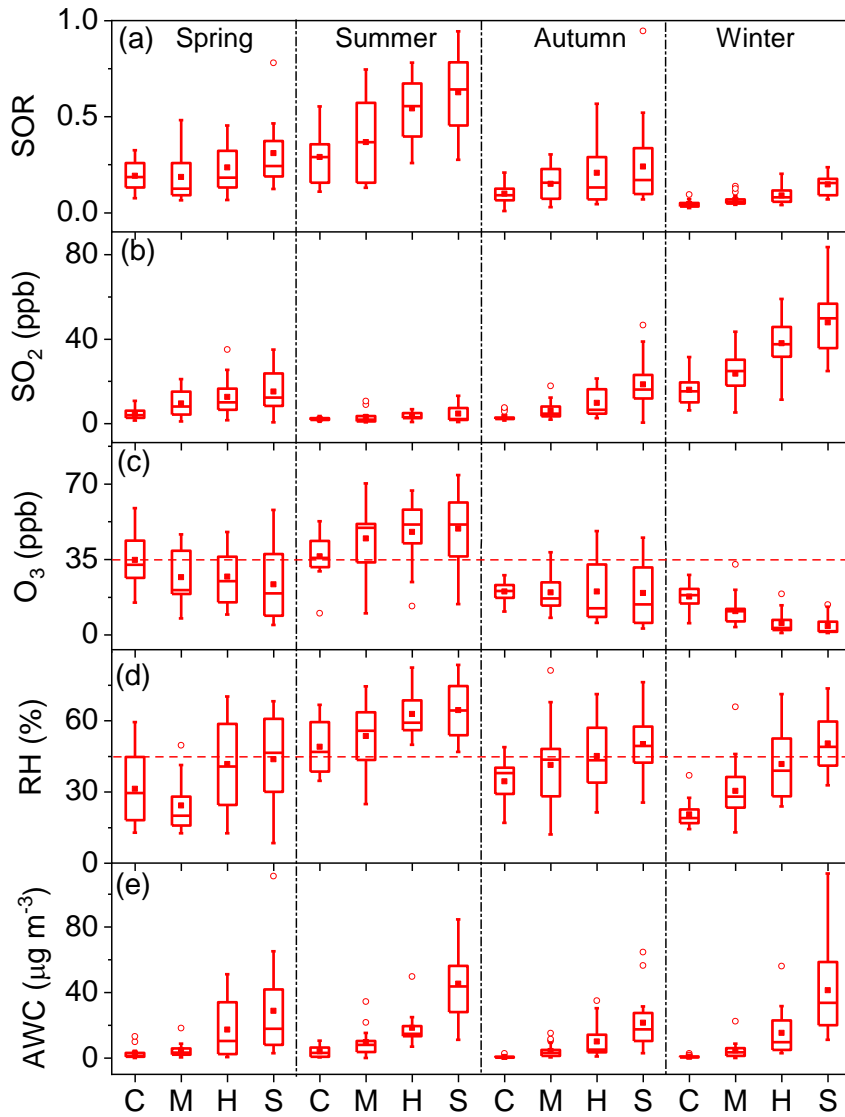
598

599 **Figure 9.** Time series of (a) SORs, (b) RH, (c) O₃, (d) SO₂, (e) aerosol water content (AWC), and (f) solar radiation from
 600 March 1 2012 to February 28 2013 (open black circles). The boxes represent, from top to bottom, the 75th, 50th, and 25th
 601 percentiles for each season. The whiskers, solid red squares, and open red circles represent 1.5 times the IQR, seasonal mean
 602 values, and outlier data points, respectively. The horizontal dashed lines in panels (b) and (c) represent thresholds of RH = 45 %
 603 and O₃ = 35 ppb, respectively.



604

605 **Figure 10.** Variations in the mean concentrations (upper panels) and contributions (lower panels) of the seven major known
 606 components of PM_{2.5} with pollution levels in each season. C, clean; M, moderate pollution; H, heavy pollution; S, severe
 607 pollution.



608

609 **Figure 11.** Variations in (a) SORs, (b) SO₂, (c) O₃, (d) RH, and (e) AWC with pollution levels in each season. C, clean; M,

610 moderate pollution; H, heavy pollution; S, severe pollution. The boxes represent, from top to bottom, the 75th, 50th, and 25th

611 percentiles for each pollution level. The whiskers, solid red squares, and open red circles represent 1.5 times the IQR, mean

612 values, and outlier data points, respectively. The horizontal dashed lines in panels (c) and (d) represent thresholds of O₃ = 35

613 ppb and RH = 45 %, respectively.

614 **Table 1.** Annual and seasonal mean concentrations ($\mu\text{g m}^{-3}$, ± 1 standard deviation) of $\text{PM}_{2.5}$ and its **seven major known**
 615 components.

Component	Annual	Spring	Summer	Autumn	Winter
$\text{PM}_{2.5}$	84.1 \pm 63.1	113.1 \pm 62.0	52.7 \pm 32.6	60.0 \pm 51.3	105.0 \pm 71.7
NH_4^+	6.4 \pm 6.4	6.7 \pm 7.3	5.9 \pm 5.0	4.5 \pm 4.8	8.4 \pm 7.4
SO_4^{2-}	12.0 \pm 12.2	12.9 \pm 12.4	13.3 \pm 11.5	7.9 \pm 8.7	14.5 \pm 14.4
NO_3^-	11.5 \pm 12.6	15.0 \pm 16.0	7.6 \pm 8.0	9.0 \pm 11.8	13.6 \pm 12.1
OM	22.7 \pm 18.1	21.5 \pm 10.5	11.1 \pm 3.8	19.2 \pm 16.1	35.2 \pm 23.4
minerals	14.7 \pm 27.0	40.7 \pm 45.0	3.7 \pm 1.6	6.5 \pm 7.0	8.0 \pm 5.6
TEOs	1.3 \pm 0.7	1.5 \pm 0.6	1.2 \pm 0.4	1.3 \pm 0.7	1.3 \pm 0.8
EC	2.1 \pm 1.5	1.9 \pm 1.0	1.1 \pm 0.5	1.9 \pm 1.3	2.9 \pm 2.0

616

617

618 **Supplementary information**

619 **S1. Methodology for estimation of the mass concentrations of PM_{2.5} components**

620 **S1.1 Organic matter**

621 The mass concentration of organic matter (OM) was calculated from organic carbon (OC) measurements
622 by multiplying OC by a factor that represents the mass contributions of other elements, such as oxygen,
623 hydrogen, and nitrogen. The OM/OC ratio varies from 1.4 to 2.2 and is expected to increase as aerosols
624 age (El-Zanan et al., 2005). We chose a factor of 1.6 to calculate OM in Beijing following advice in the
625 literature (Xing et al., 2013).

626 **S1.2 Minerals**

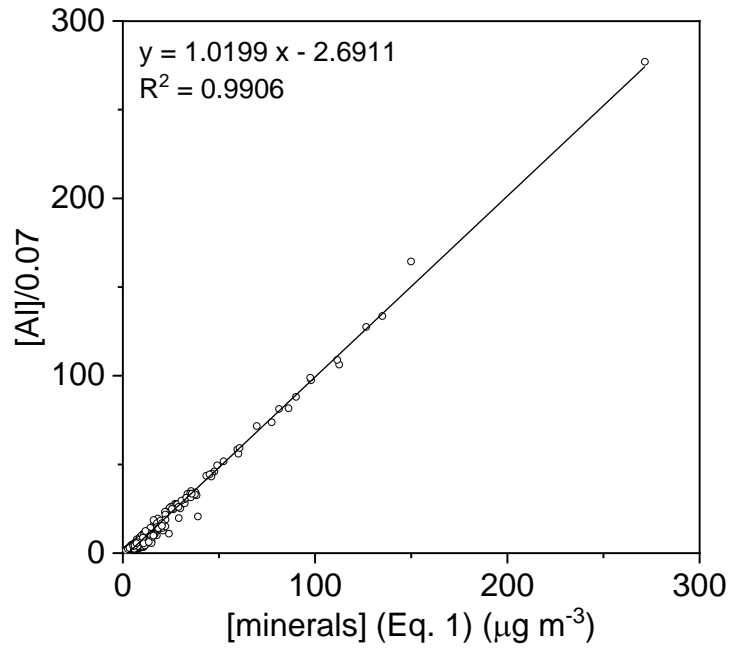
627 The total mass concentration of minerals, referred to as “minerals”, can be estimated by the following
628 equation (Chan et al., 1997):

$$629 [\text{minerals}] = 2.2[\text{Al}] + 2.49[\text{Si}] + 1.63[\text{Ca}] + 2.42[\text{Fe}] + 1.94[\text{Ti}] \quad , \quad (\text{Eq. 1})$$

630 where $[x]$ represents the mass concentration of species x . According to Zhang et al. (2003), on average Al
631 accounted 7 % of total mineral dust mass concentrations in North, Northwest, and West China. Mineral
632 concentrations can thus also be estimated by Eq. 2:

$$633 [\text{minerals}] = [\text{Al}]/0.07 \quad , \quad (\text{Eq. 2})$$

634 We calculated [minerals] with the two methods above and found no significant differences (Fig. S1).
635 Equation 2 was therefore employed to calculate [minerals] in this study.



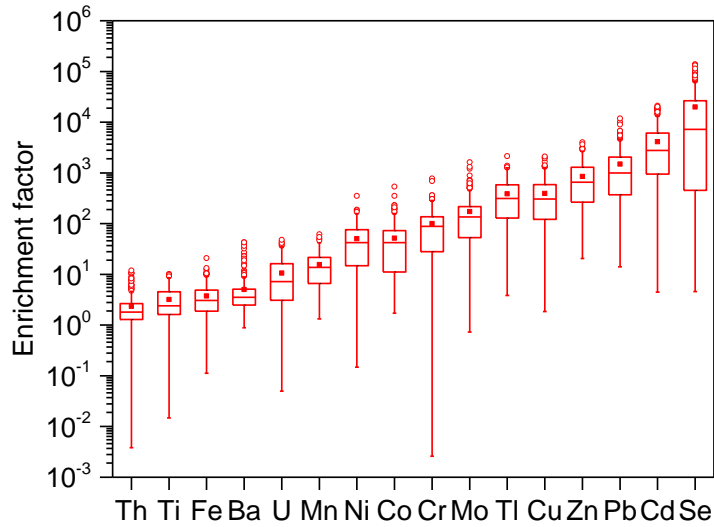
636
637 **Figure S1.** Comparison of the two methods for the calculation of [minerals].

638 **S1.3 Trace element oxides**

639 The enrichment factors (EFs) of trace element oxides (TEOs) can be used to determine whether natural
640 or anthropogenic sources dominated our observations. The EF value of element i was defined as follows:

$$641 \text{EF}_i = \frac{[X_i/X_{\text{ref}}]_{\text{sample}}}{[X_i/X_{\text{ref}}]_{\text{crust}}}, \quad (\text{Eq. 3})$$

642 where $[X_i/X_{\text{ref}}]_{\text{sample}}$ is the mass concentration ratio of element i to the reference element in our samples
643 and $[X_i/X_{\text{ref}}]_{\text{crust}}$ is the mass concentration ratio of element i to the reference element in average crust (Hans
644 Wedepohl, 1995). Al was used as the reference element in this study. The EFs of each element are depicted
645 in Fig. S2.



646
 647 **Figure S2.** Elemental enrichment factors (EFs) of our samples. The boxes represent, from top to bottom, the 75th, 50th, and
 648 25th percentiles for each element. The whiskers, solid red squares, and open red circles represent 1.5 times the interquartile
 649 range (IQR), mean values, and outlier data points, respectively.

650 If the EF was < 5 , the element was considered to originate mainly from natural sources; if $5 < EF < 20$,
 651 the element originated from both natural and anthropogenic sources; if $EF > 20$, the element originated
 652 mainly from anthropogenic sources. According to Zhang et al. (2013), the mass concentrations of TEOs
 653 can be estimated by multiplied a **correction** factor to represent the contribution of oxygen. For elements
 654 originating from anthropogenic sources only, a factor of 1 was applied, whereas for elements of both
 655 natural and anthropogenic origin, a factor of 0.5 was applied to represent the anthropogenic part. As
 656 multiple forms of metal oxides were identified, which were hard to quantify, a multiplicative factor of 1.3
 657 was used when considering the metal abundance. The mass concentration of TEOs was calculated as
 658 described in Zhang et al. (2013):

659
$$[\text{TEOs}] = 1.3 \times [0.5 \times (\text{Ba} + \text{Mn} + \text{U}) + (\text{Ni} + \text{Co} + \text{Cr} + \text{Mo} + \text{Tl} + \text{Cu} + \text{Zn} + \text{Pb} + \text{Cd} + \text{Se})]$$
 , (Eq. 4)

660 **S1.4 Aerosol water content**

661 Aerosol water content (AWC) was calculated using the ISORROPIA-II thermodynamic model
 662 (<http://isorro피아.eas.gatech.edu>). The $\text{Na}^+ - \text{K}^+ - \text{Ca}^{2+} - \text{Mg}^{2+} - \text{NH}_4^+ - \text{SO}_4^{2-} - \text{NO}_3^- - \text{Cl}^- - \text{H}_2\text{O}$ aerosol system
 663 was applied in reverse mode (Fountoukis and Nenes, 2007; Nenes et al., 1998).

664 S2 Results and discussion

665 S2.1 Sulfate formation mechanism

666 Sulfate can be formed through the oxidation of SO₂ by OH radicals in the gas phase (Stockwell and
667 Calvert, 1983), through the oxidation of dissolved SO₂ by various oxidants (e.g., O₃, H₂O₂, NO₂, and O₂)
668 in the aqueous phase (Seinfeld and Pandis, 2006), which may be transition metal ions (TMIs)-catalysed,
669 or through heterogeneous reaction on the surface of sea-salt or dust aerosols (Gurciullo et al., 1999; Usher,
670 2002).

671 The rate of the SO₂ + OH reaction can be expressed as:

$$672 R_{\text{SO}_2+\text{OH}} = k_0[\text{SO}_2(\text{g})][\text{OH}(\text{g})] \quad , \quad (\text{Eq. 5})$$

673 where k_0 is the rate constant and $[x]$ represents the concentration of species x . The production rate of
674 sulfate through OH radical oxidation can be expressed as:

$$675 P_{\text{OH}} = \frac{3600 \times 96 \times p \times R_{\text{SO}_2+\text{OH}}}{RT} \quad , \quad (\text{Eq. 6})$$

676 where 3600 is a time conversion factor (s h⁻¹), 96 is the molar mass of SO₄²⁻ (g mol⁻¹), p is atmospheric
677 pressure (kPa), R is the gas constant (8.31 Pa m³ mol⁻¹ K⁻¹), and T is the temperature (K).

678 SO₂ reacts with H₂O₂, O₃, NO₂, and O₂ (TMIs-catalysed) in the aqueous phase. The rates of the four main
679 aqueous reactions are expressed as (He et al., 2018; Seinfeld and Pandis, 2006):

$$680 R_{\text{SO}_2+\text{O}_3} = (k_1[\text{SO}_2 \cdot \text{H}_2\text{O}] + k_2[\text{HSO}_3^-] + k_3[\text{SO}_3^{2-}])[\text{O}_3(\text{aq})] \quad , \quad (\text{Eq. 7})$$

$$681 R_{\text{SO}_2+\text{H}_2\text{O}_2} = \frac{k_4[\text{H}^+][\text{HSO}_3^-][\text{H}_2\text{O}_2(\text{aq})]}{1 + K[\text{H}^+]} \quad , \quad (\text{Eq. 8})$$

$$682 R_{\text{SO}_2+\text{NO}_2} = k_5[\text{S(IV)}][\text{NO}_2(\text{aq})] \quad , \quad (\text{Eq. 9})$$

$$683 R_{\text{SO}_2+\text{O}_2} = k_6[\text{H}^+]^{-0.74} [\text{S(IV)}][\text{Mn(II)}][\text{Fe(III)}] \quad (\text{pH} < 4.2) \quad , \quad (\text{Eq. 10})$$

$$684 R_{\text{SO}_2+\text{O}_2} = k_7[\text{H}^+]^{0.67} [\text{S(IV)}][\text{Mn(II)}][\text{Fe(III)}] \quad (\text{pH} > 4.2) \quad , \quad (\text{Eq. 11})$$

685 The production rate of sulfate through aqueous oxidation routes can be expressed as:

$$686 P_{\text{aqu}(\text{ox}_i)} = 3600 \times 96 \times R_{\text{SO}_2+\text{ox}_i} \times \frac{\text{LWC}}{\rho_{\text{H}_2\text{O}}} \quad , \quad (\text{Eq. 12})$$

687 where k_n ($n = 1-7$) is the rate constant of each oxidation route, $K = 13 \text{ M}^{-1}$ at 298 K, LWC is the liquid
688 water content (mg m⁻³), $\rho_{\text{H}_2\text{O}}$ is the density of water (1 kg L⁻¹), and ox _{i} ($i = \text{O}_3, \text{H}_2\text{O}_2, \text{NO}_2, \text{and O}_2$)
689 represents different oxidants.

690 The heterogeneous reaction rate $R_{\text{het}(\text{ox}_i)}$ can be expressed as (Jacob, 2000; Wang et al., 2012; Zheng et

691 al., 2015):

$$692 \quad R_{\text{het}(\text{ox}_i)} = k_{\text{ox}_i} [\text{SO}_2(\text{g})] \quad , \quad (\text{Eq. 13})$$

693 where

$$694 \quad k_{\text{ox}_i} = \left(\frac{d_p}{2D_i} + \frac{4}{v_i \gamma_i} \right)^{-1} S_p \quad , \quad (\text{Eq. 14})$$

695 d_p is the effective diameter of the particles (m), D_i is the gas phase molecular diffusion coefficient (m^2
696 s^{-1}), v_i is the mean molecular speed in the gas phase (m s^{-1}), and S_p is the aerosol surface area ($\text{m}^2 \text{m}^{-3}$).

697 The uptake coefficient γ_i depends on RH:

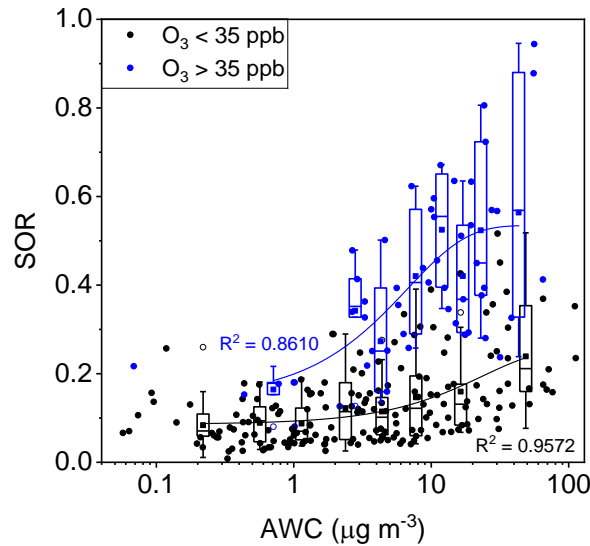
$$698 \quad \gamma_i = \left\{ \begin{array}{ll} \gamma_{\text{low}} & 0 < \text{RH} \leq 50 \% \\ \gamma_{\text{low}} + \frac{(\gamma_{\text{high}} - \gamma_{\text{low}})(\text{RH} - 0.5)}{\text{RH}_{\text{max}} - 0.5} & 50 \% < \text{RH} \leq \text{RH}_{\text{max}} \\ \gamma_{\text{high}} & \text{RH}_{\text{max}} < \text{RH} \leq 100 \% \end{array} \right\} \quad (\text{Eq. 15})$$

699 where γ_{low} and γ_{high} can be obtained from Wang et al. (2012) and RH_{max} is the RH at which γ reaches γ_{high} .

700 The rate of sulfate production via heterogeneous reactions $P_{\text{het}(\text{ox}_i)}$ can be expressed as:

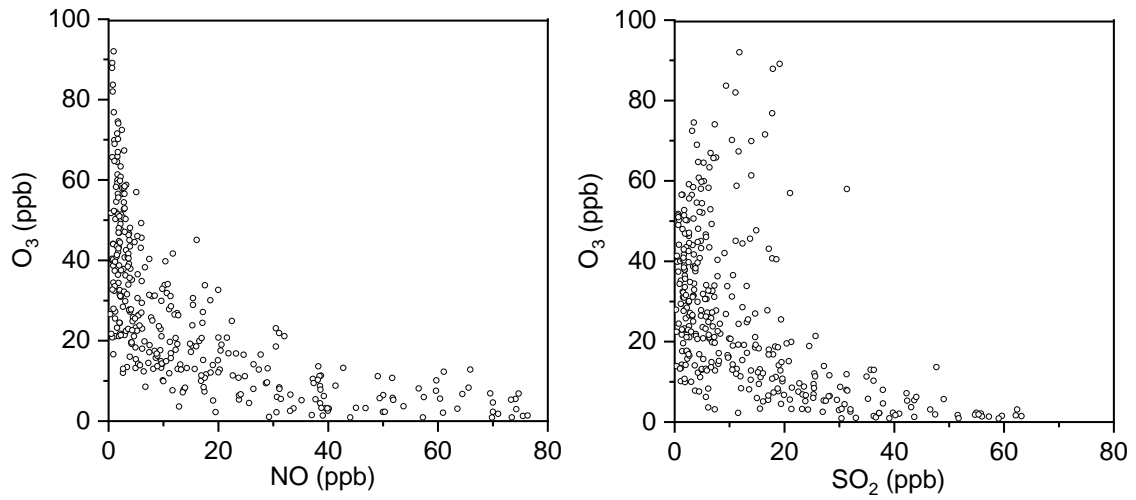
$$701 \quad P_{\text{het}(\text{ox}_i)} = \frac{3600 \times 96 \times p \times R_{\text{het}(\text{ox}_i)}}{RT} \quad , \quad (\text{Eq. 16})$$

702 **S2.2 Influencing parameters**

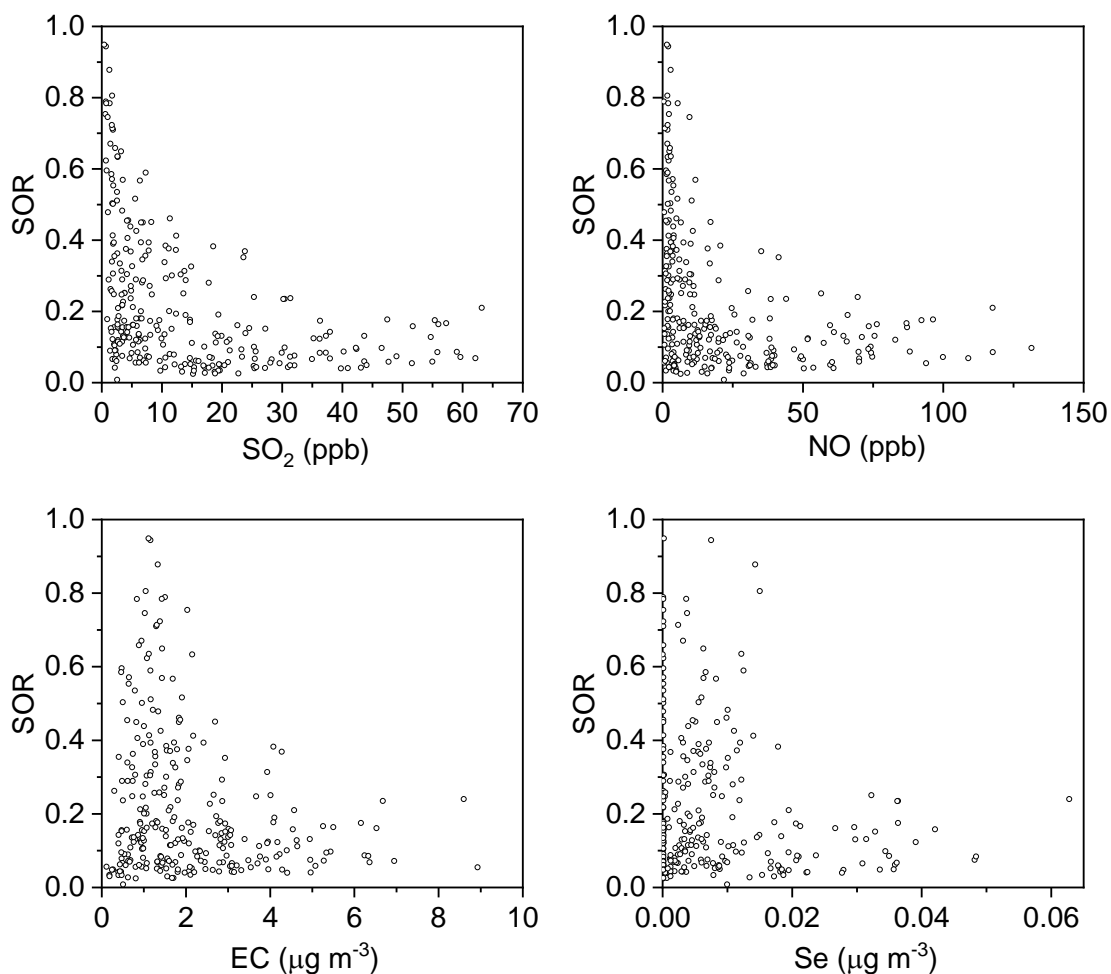


703 **Figure S3.** Plot of the SOR against aerosol water content (AWC) (note log scale), grouped by O_3 concentration. The solid blue
704 circles represent $\text{O}_3 > 35$ ppb and the solid black circles represent $\text{O}_3 < 35$ ppb. The boxes represent, from top to bottom, the
705 75th, 50th, and 25th percentiles in each bin, which were also separated according to the 35 ppb O_3 concentration threshold; the
706

707 bin widths were set such that there were an approximately equal number of data points in each bin. The whiskers, solid squares,
708 and open circles represent 1.5 times the IQR, mean values, and outlier data points, respectively. The lines are best fits to the
709 mean values based on a sigmoid function. Data for days with rain or snow were excluded from this plot.



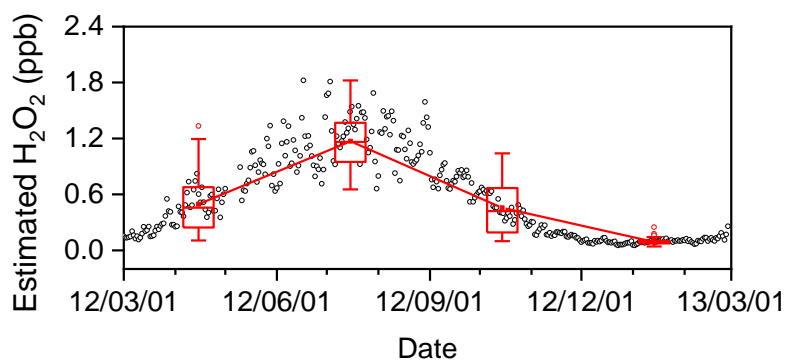
710
711 **Figure S4.** Plots of O₃ against the primary emission tracers NO and SO₂.



712

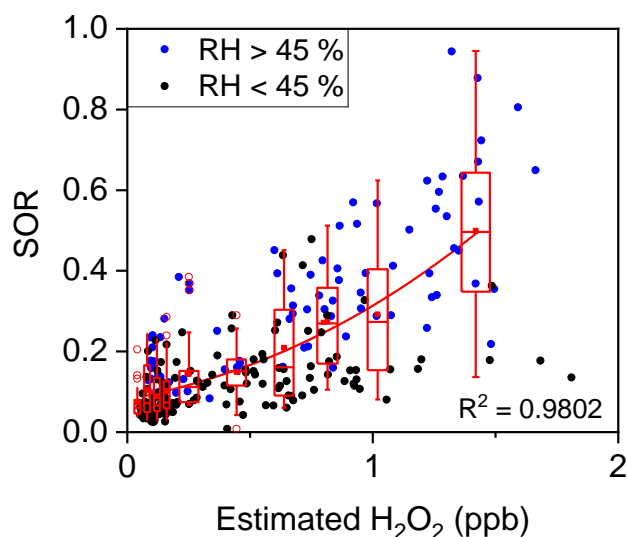
713 **Figure S5.** Plots of sulfur oxidation ratios (SORs) against the primary emission tracers SO₂, NO, EC, and Se.

714



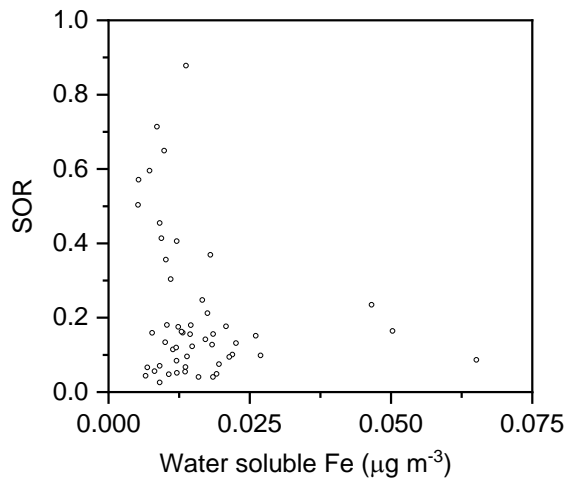
715

716 **Figure S6.** Time series of estimated H₂O₂ from March 1 2012 to February 28 2013. H₂O₂ was estimated from temperature (T)
 717 based on the fitting function $H_2O_2 = 0.1155e^{0.0846T}$ according to Fu (2014). The boxes represent, from top to bottom, the 75th,
 718 50th, and 25th percentiles for each season. The whiskers, solid red squares, and open red circles represent 1.5 times the
 719 interquartile range (IQR), seasonal mean values, and outlier data points, respectively.



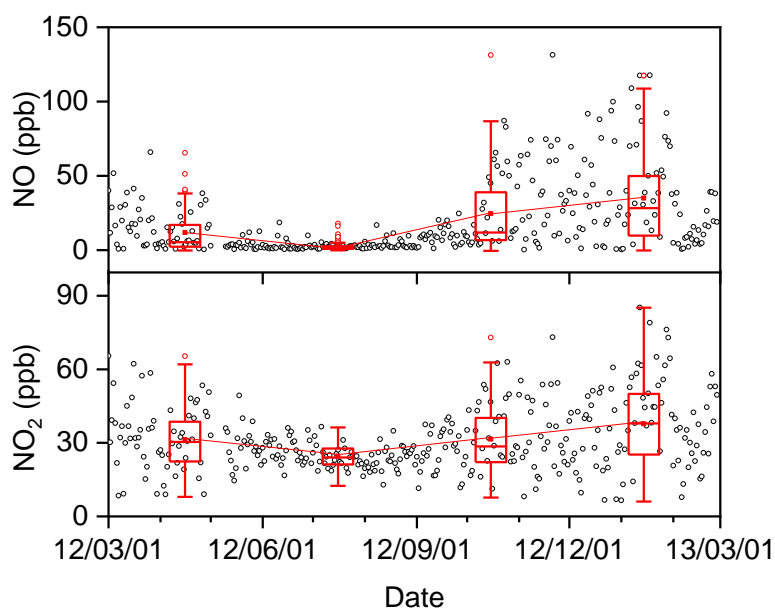
720

721 **Figure S7.** Plot of the SOR against estimated H_2O_2 grouped by RH. The solid blue circles represent $\text{RH} > 45\%$ and the solid
 722 black circles represent $\text{RH} < 45\%$. The boxes represent, from top to bottom, the 75th, 50th, and 25th percentiles in each bin. The
 723 bin widths were set such that there were an approximately equal number of data points in each bin. The whiskers, solid squares,
 724 and open circles represent 1.5 times the IQR, mean values, and outlier data points, respectively. The line are best fits to the
 725 mean values based on an exponential function. Data for days with rain were excluded from this plot.



726

727 **Figure S8.** Plot of the SOR against water soluble Fe (54 samples selected every 6 days throughout the sampling period).



729

730 **Figure S9.** Time series of NO and NO₂ from March 1 2012 to February 28 2013 (open black circles). The boxes represent,
 731 from top to bottom, the 75th, 50th, and 25th percentiles for each season. The whiskers, solid red squares, and open red circles
 732 represent 1.5 times the IQR, seasonal mean values, and outlier data points, respectively.

733 References

- 734 Chan, Y. C., Simpson, R. W., McTainsh, G. H., Vowles, P. D., Cohen, D. D., and Bailey, G. M.:
 735 Characterisation of chemical species in PM_{2.5} and PM₁₀ aerosols in Brisbane, Australia, *Atmos.*
 736 *Environ.*, 31, 3773-3785, [https://doi.org/10.1016/S1352-2310\(02\)00804-X](https://doi.org/10.1016/S1352-2310(02)00804-X), 1997.
- 737 El-Zanan, H. S., Lowenthal, D. H., Zielinska, B., Chow, J. C., and Kumar, N.: Determination of the
 738 organic aerosol mass to organic carbon ratio in IMPROVE samples, *Chemosphere*, 60, 485-496,
 739 <https://doi.org/10.1016/j.chemosphere.2005.01.005>, 2005.
- 740 Fountoukis, C., and Nenes, A.: ISORROPIA II: a computationally efficient thermodynamic equilibrium
 741 model for K⁺-Ca²⁺-Mg²⁺-NH₄⁺-Na⁺-SO₄²⁻-NO₃⁻-Cl⁻-H₂O aerosols, *Atmos. Chem. Phys.*, 7, 4639-
 742 4659, <https://doi.org/10.5194/acp-7-4639-2007>, 2007.
- 743 Fu, A.: Study on peroxide concentration and its influence factors in the urban atmosphere, Master, College
 744 of Environmental and Resource Sciences, Zhejiang University, Hangzhou, China, 2014 (in Chinese).
- 745 Gurciullo, C., Lerner, B., Sievering, H., and Pandis, S. N.: Heterogeneous sulfate production in the remote

746 marine environment: Cloud processing and sea-salt particle contributions, *J. Geophys. Res.*, 104, 21719,
747 <https://doi.org/10.1029/1999jd900082>, 1999.

748 Hans Wedepohl, K.: The composition of the continental crust, *Geochim. Cosmochim. Ac*, 59, 1217-1232,
749 [https://doi.org/10.1016/0016-7037\(95\)00038-2](https://doi.org/10.1016/0016-7037(95)00038-2), 1995.

750 He, P., Alexander, B., Geng, L., Chi, X., Fan, S., Zhan, H., Kang, H., Zheng, G., Cheng, Y., Su, H., Liu,
751 C., and Xie, Z.: Isotopic constraints on heterogeneous sulfate production in Beijing haze, *Atmos. Chem.*
752 *Phys.*, 18, 5515-5528, <https://doi.org/10.5194/acp-18-5515-2018>, 2018.

753 Jacob, D. J.: Heterogeneous chemistry and tropospheric ozone, *Atmos. Environ.*, 34, 2131-2159,
754 [https://doi.org/10.1016/s1352-2310\(99\)00462-8](https://doi.org/10.1016/s1352-2310(99)00462-8), 2000.

755 Nenes, A., Pandis, S. N., and Pilinis, C.: ISORROPIA: A new thermodynamic equilibrium model for
756 multiphase multicomponent inorganic aerosols, *Aquat. Geochem.*, 4, 123-152,
757 <https://doi.org/10.1023/a:1009604003981>, 1998.

758 Seinfeld, J. H., and Pandis, S. N.: *Atmospheric chemistry and physics: From air pollution to climate*
759 *change*, second ed., John Wiley & Sons, New Jersey, 2006.

760 Stockwell, W. R., and Calvert, J. G.: The mechanism of the HO-SO₂ reaction, *Atmos. Environ.*, 17, 2231-
761 2235, [https://doi.org/10.1016/0004-6981\(83\)90220-2](https://doi.org/10.1016/0004-6981(83)90220-2), 1983.

762 Usher, C. R.: A laboratory study of the heterogeneous uptake and oxidation of sulfur dioxide on mineral
763 dust particles, *J. Geophys. Res.*, 107, <https://doi.org/10.1029/2002JD002051>, 2002.

764 Wang, K., Zhang, Y., Nenes, A., and Fountoukis, C.: Implementation of dust emission and chemistry into
765 the Community Multiscale Air Quality modeling system and initial application to an Asian dust storm
766 episode, *Atmos. Chem. Phys.*, 12, 10209-10237, <https://doi.org/10.5194/acp-12-10209-2012>, 2012.

767 Xing, L., Fu, T. M., Cao, J. J., Lee, S. C., Wang, G. H., Ho, K. F., Cheng, M. C., You, C. F., and Wang, T.
768 J.: Seasonal and spatial variability of the OM/OC mass ratios and high regional correlation between
769 oxalic acid and zinc in Chinese urban organic aerosols, *Atmos. Chem. Phys.*, 13, 4307-4318,
770 <https://doi.org/10.5194/acp-13-4307-2013>, 2013.

771 Zhang, R., Jing, J., Tao, J., Hsu, S. C., Wang, G., Cao, J., Lee, C. S. L., Zhu, L., Chen, Z., Zhao, Y., and
772 Shen, Z.: Chemical characterization and source apportionment of PM_{2.5} in Beijing: Seasonal
773 perspective, *Atmos. Chem. Phys.*, 13, 7053-7074, <https://doi.org/10.5194/acp-13-7053-2013>, 2013.

774 Zhang, X. Y., Gong, S. L., Shen, Z. X., Mei, F. M., Xi, X. X., Liu, L. C., Zhou, Z. J., Wang, D., Wang, Y.
775 Q., and Cheng, Y.: Characterization of soil dust aerosol in China and its transport and distribution

776 during 2001 ACE-Asia: 1. Network observations, *J. Geophys. Res.*, 108,
777 <https://doi.org/10.1029/2002jd002632>, 2003.

778 Zheng, B., Zhang, Q., Zhang, Y., He, K. B., Wang, K., Zheng, G. J., Duan, F. K., Ma, Y. L., and Kimoto,
779 T.: Heterogeneous chemistry: a mechanism missing in current models to explain secondary inorganic
780 aerosol formation during the January 2013 haze episode in North China, *Atmos. Chem. Phys.*, 15, 2031-
781 2049, <https://doi.org/10.5194/acp-15-2031-2015>, 2015.